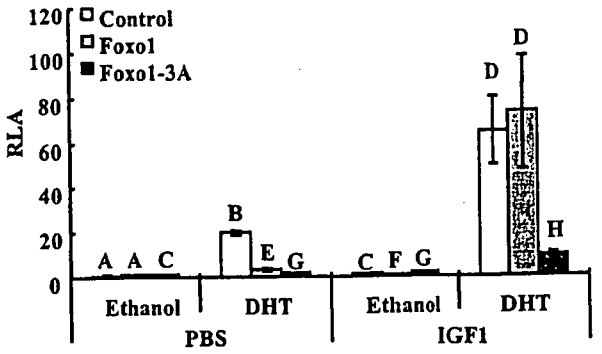

FIGURE 2. **IGF1 ameliorates Foxo1-suppressed AR transactivation.** LNCaP cells growing in 24-well plates were cotransfected with 100 ng of FLAG-Foxo1, FLAG-Foxo1-3A (Akt-nonphosphorylatable constitutively active mutant), or an equimolar amount of pcDNA-FLAG together with 400 ng of PSA-Luc, 5 ng of pRL-CMV, 40 ng of PTEN, and 40 ng of pCMV-hAR. At 48 h post-transfection, the cells were exposed to 10^{-8} M DHT and/or 100 ng/ml IGF1 in serum-free medium for 24 h, before being lysed and analyzed by luciferase assays. *Letters above the bars* show statistical groups (ANOVA, $p < 0.05$). The ascending order of the groups is as follows: F, A, C, G, E, H, B, and D. *RLA*, relative luciferase activity.

LNCaP cells in a concentration-dependent manner, albeit less potently (supplemental Fig. 3*b*).

To exclude the possibility that Foxo1 inhibits AR transactivation by decreasing the protein level of the receptor, the AR protein level was examined by immunoblotting under the same conditions used for the reporter assays. As shown in supplemental Fig. 4, *a–c*, cotransfection of Foxo1 with AR into LNCaP cells did not alter the AR protein level in either the presence or absence of DHT. Similarly, the AR mRNA expression level in lentiviral Foxo1-infected LNCaP cells was not significantly altered (supplemental Fig. 4*d*). Hence, these data indicate that Foxo1 suppresses the specific activity of the receptor.

Physical Interaction between Foxo1 and AR—Next, we examined whether there is a direct physical interaction between AR and Foxo1 by using coimmunoprecipitation assays. LNCaP cells cotransfected with FLAG-Foxo1 and pCMV-hAR together with PTEN and grown in serum-free medium were treated with IGF1, insulin, or PBS in combination with DHT or ethanol. As shown in Fig. 3*a* (*upper panel*), FLAG-Foxo1 bands were detected in anti-AR antibody-precipitated immune complexes from cells treated with DHT (*lanes 6–8*), whereas a very weak signal was detected in ethanol-treated cells (*lane 2*), suggesting that Foxo1 and AR interact directly, and their interaction is significantly enhanced by the AR ligand. The presence of IGF1 or insulin did not abolish the interaction (Fig. 3*a* (*upper panel*), *lanes 7* and *8*), although both molecules appeared to reduce the amount of Foxo1 protein interacting with liganded AR. In contrast, no Foxo1 signal was detectable in normal rabbit IgG-precipitated immune complexes from cells treated with either ethanol (Fig. 3*a* (*upper panel*), *lane 1*) or DHT (*lane 5*), indicating the specificity of the Foxo1-AR interaction. Using PTEN-expressing LNCaP cells, we further verified that endogenous AR and Foxo1 interacted in an androgen-dependent manner (supplemental Fig. 5), suggesting that the observed interaction is physiologically meaningful and that Foxo1 may repress liganded activated AR via a direct protein-protein interaction.

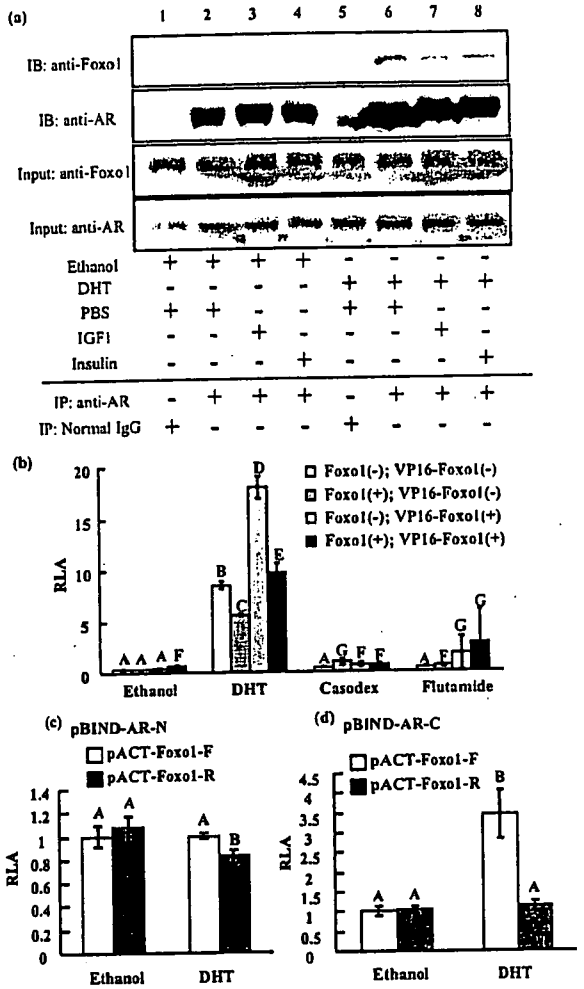

FIGURE 3. **Physical interaction between Foxo1 and AR.** *a*, coimmunoprecipitation of AR with Foxo1. LNCaP cells transfected with PTEN, pCMV-hAR, and pcDNA-FLAG-Foxo1 or the control empty vector pcDNA-FLAG were treated with PBS, IGF1 (100 ng/ml), or insulin (10 μg/ml) in combination with DHT (10^{-8} M) or ethanol as indicated. Aliquots (1000 μg) of whole cell extracts were incubated with 5 μg of rabbit anti-AR (N-20) antibody or control normal rabbit IgG together with 50 μl of protein A beads, and the presence of FLAG-Foxo1 in the immunoprecipitates (*IP*) was detected by immunoblotting (*IB*) with an anti-Foxo1 mouse monoclonal antibody. Immunoprecipitation of AR by the anti-AR (N-20) antibody was validated by using an anti-AR antibody obtained from Cell Signaling (catalog number 3202). The presence of AR and Foxo1 in the input cell lysate samples were confirmed. *b*, modified one-hybrid assays. COS7 cells were cotransfected with 50 ng of vectors for Foxo1 (pcDNA-FLAG-Foxo1), VP16-Foxo1 fusion protein (pACT-Foxo1), or both together with 300 ng of pGL3-MMTV, 5 ng of pRL-CMV, and 50 ng of pCMV-hAR and subsequently treated with 10^{-8} M DHT, 10^{-6} M casodex, 10^{-6} M hydroxyflutamide, or the solvent (ethanol), respectively, for 24 h, before being analyzed by luciferase assays. Note that the DHT-induced AR transactivation is inhibited by Foxo1 but enhanced by VP16-Foxo1. The ascending order of the groups is A, F, G, C, B, E, and D. *c* and *d*, the C terminus of AR mediates the interaction with Foxo1. Mammalian two-hybrid assays were carried out to test for an *in vivo* interaction between AR and Foxo1. COS7 cells were cotransfected with a DNA mixture consisting of 100 ng of pG5-LUC, 1.5 ng of pRL-CMV, and 75 ng of pACT-Foxo1 together with 25 ng of pBIND-AR-N (*c*) or equimolar amounts of pBIND-AR-C (*d*). After the transfection, the cells were treated with 10^{-8} M DHT or ethanol. Parallel experiments in which pACT-Foxo1 was replaced with pACT-Foxo1-R (Foxo1 fused with VP16 in the reverse orientation) were carried out as controls. *Letters above the bars* show statistical groups (ANOVA, $p < 0.05$). *RLA*, relative luciferase activity.

The interaction was further confirmed by modified mammalian one-hybrid assays (29). COS7 cells were cotransfected with an MMTV reporter and AR together with wild-type Foxo1,

pACT-Foxo1, or both, and then treated with DHT or two antiandrogens, namely hydroxyflutamide and casodex. As shown in Fig. 3*b*, FLAG-Foxo1 inhibited DHT-induced AR transactivation as expected. However, pACT-Foxo1 (with a viral VP16 activation domain fused to the Foxo1 N terminus) enhanced the liganded AR function, and the coexistence of FLAG-Foxo1 and pACT-Foxo1 neutralized the luciferase activity. Thus, although Foxo1 was suppressive toward AR, VP16-Foxo1 became an artificial coactivator for AR, and this remarkable shift strongly suggests that there is a direct interaction between AR and Foxo1. Interestingly, the antiandrogens casodex and hydroxyflutamide did not produce the same phenomenon, suggesting that only an agonist can induce the interaction.

Further clarification of the individual domains of AR responsible for the interaction with Foxo1 was carried out by mammalian two-hybrid assays, in which the AR N terminus (amino acids 1–660) and C terminus (amino acids 615–919) were individually fused to the DNA-binding domain of GAL4 to produce pBIND-AR-N and pBIND-AR-C, respectively. As a control, the full-length Foxo1 cDNA was fused to the VP16 activation domain in either the forward (pACT-Foxo1-F) or reverse orientation (pACT-Foxo1-R). In comparison with pACT-Foxo1-R, pACT-Foxo1-F did not alter the activity of the pG5-LUC reporter coexpression with pBIND-AR-N in either the presence or absence of the ligand, suggesting a lack of interaction between the AR N terminus and Foxo1 (Fig. 3*c*). In the case of pBIND-AR-C coexpression, pACT-Foxo1-F, but not pACT-Foxo1-R, significantly stimulated the reporter in the presence of DHT (Fig. 3*d*). These data indicate that the AR C terminus interacts with Foxo1 in a hormone-dependent manner.

Subcellular Interactions between Foxo1 and AR in Living Cells—The intracellular distribution of EYFP-Foxo1 in living COS7 cells was visualized using laser confocal scanning microscopy. Consistent with previous observations (17), EYFP-Foxo1 in serum-starved COS7 cells was predominantly located in the nucleus in a homogeneous manner, with relatively weak diffuse fluorescence also visible in the cytoplasm (Fig. 4*a*). However, the nuclear accumulation of Foxo1 varied among the examined cells (supplemental Fig. 6, *a–c*). This variation was presumably because of differing IGF1/insulin signaling tones among the different cells, because challenge with IGF1 caused 100% of the EYFP-Foxo1-expressing cells to show complete cytoplasmic fluorescence (Fig. 4*b*). As expected, EGFP-AR predominantly showed diffuse fluorescence in the cytosol with very weak nuclear fluorescence in the absence of the ligand (Fig. 4*c*), whereas DHT induced complete nuclear translocation and typical subnuclear foci formation (Fig. 4*d*). When EYFP-Foxo1 and EGFP-AR were coexpressed, both proteins showed their original distribution patterns in cells treated with the control solvents (IGF1−/DHT−; Fig. 4*f*). Among the cells treated with DHT alone (IGF1−/DHT−; Fig. 4*g*), the distribution of EYFP-Foxo1 remained almost unchanged, whereas EGFP-AR exhibited incomplete nuclear translocation and significantly impaired subnuclear compartmentalization (foci formation) and was diffuse in both the nucleus and cytoplasm. Although a subgroup of cells showed relatively complete nuclear translocation, their foci formation was apparently impaired (supplemental Fig. 6*d*). In cells treated with IGF1 alone (IGF1+/DHT−; Fig. 4*i*), EYFP-Foxo1 was completely exported to the cytoplasm, whereas EGFP-AR maintained its original distribution, namely predominant diffuse cytoplasmic localization with weak nuclear fluorescence. In comparison with IGF1−/DHT+ cells (Fig. 4*g*), EGFP-AR in cells treated with both ligands (IGF1+/DHT+; Fig. 4*j*) showed more complete nuclear translocation and, importantly, also exhibited significantly improved subnuclear compartmentalization.

To quantitatively evaluate the effects of IGF1/Foxo1 on the subnuclear distribution of liganded AR, the intranuclear distribution patterns of EGFP-AR in the cell populations, shown representatively in Fig. 4, *d*, *g*, and *j*, were subjected to line scan analyses using the LSM software as described previously (22). In Fig. 4, *e*, *h*, and *k* show the line scan data of *d*, *g*, and *j*, respectively. In total, 20 cells from each group were subjected to the line scan analyses. The fluorescence intensity of the cells in Fig. 4*d* was quite heterogeneous (heterogeneity index (HI) = 53.12 ± 10.53), whereas cotransfection of Foxo1 (*cells* in Fig. 4*g*) decreased the HI to 17.83 ± 9.46, indicating that the AR distribution in these cells was quite constant. The HI value recovered to 35.16 ± 18.89 in cells further treated with IGF1 (*cells* in Fig. 4*j*), suggesting that the Foxo1-inhibited subnuclear reorganization of liganded AR was partially rescued by IGF1.

3T3-L1 cells contain a relatively high quantity of endogenous AR, which undergoes typical subnuclear reorganization and forms fine foci in the presence of DHT (23). To address whether Foxo1 also suppresses the foci formation of endogenous AR, EYFP-Foxo1 was expressed in 3T3-L1 cells, and the endogenous AR distributions in the presence and absence of DHT were studied by immunofluorescence staining. As shown in supplemental Fig. 7, DHT-induced AR foci were significantly suppressed by Foxo1 overexpression. Specifically, the HI of liganded nuclear AR was 66.26 ± 15.77 ($n = 20$) in the absence of Foxo1 but reduced to 38.25 ± 8.91 ($n = 20$, $p < 0.01$) by Foxo1.

The distribution of EYFP-Foxo1 in cells coexpressing EGFP-AR and treated with both ligands (IGF1+/DHT+) was striking in that a substantial amount of Foxo1 remained in the nucleus (Fig. 4*j* and supplemental Fig. 6*e*). This distribution is in great contrast to that in the cells in Fig. 4, *b* and *i*, where IGF1 induced complete nuclear export of Foxo1 in all cells. These observations suggest that liganded AR sequestered part of the Foxo1 in the nucleus, even in the presence of IGF1. Furthermore, the nuclear Foxo1 in these cells was heterogeneous and colocalized with ligand-bound AR (Fig. 4*j* and supplemental Fig. 6*e*), suggesting an interaction between the two proteins.

In contrast to EYFP-Foxo1, EYFP-Foxo1-3A resided in the nucleus in a reticular manner regardless of the IGF1 availability. Furthermore, it disrupted DHT-induced AR foci formation, and importantly, the disruption was not rescued by IGF1 (supplemental Fig. 8).

Interaction of Foxo1 and AR within the Human PSA Promoter—Next, ChIP assays were carried out to determine whether Foxo1 and AR associate with the chromatin of an AR target gene promoter *in vivo*. LNCaP cells cotransfected with pcDNA-FLAG-Foxo1 and pCMV-hAR were subjected to serum starvation and challenged with IGF1, insulin, or PBS as a control in the presence of DHT or the solvent (ethanol).

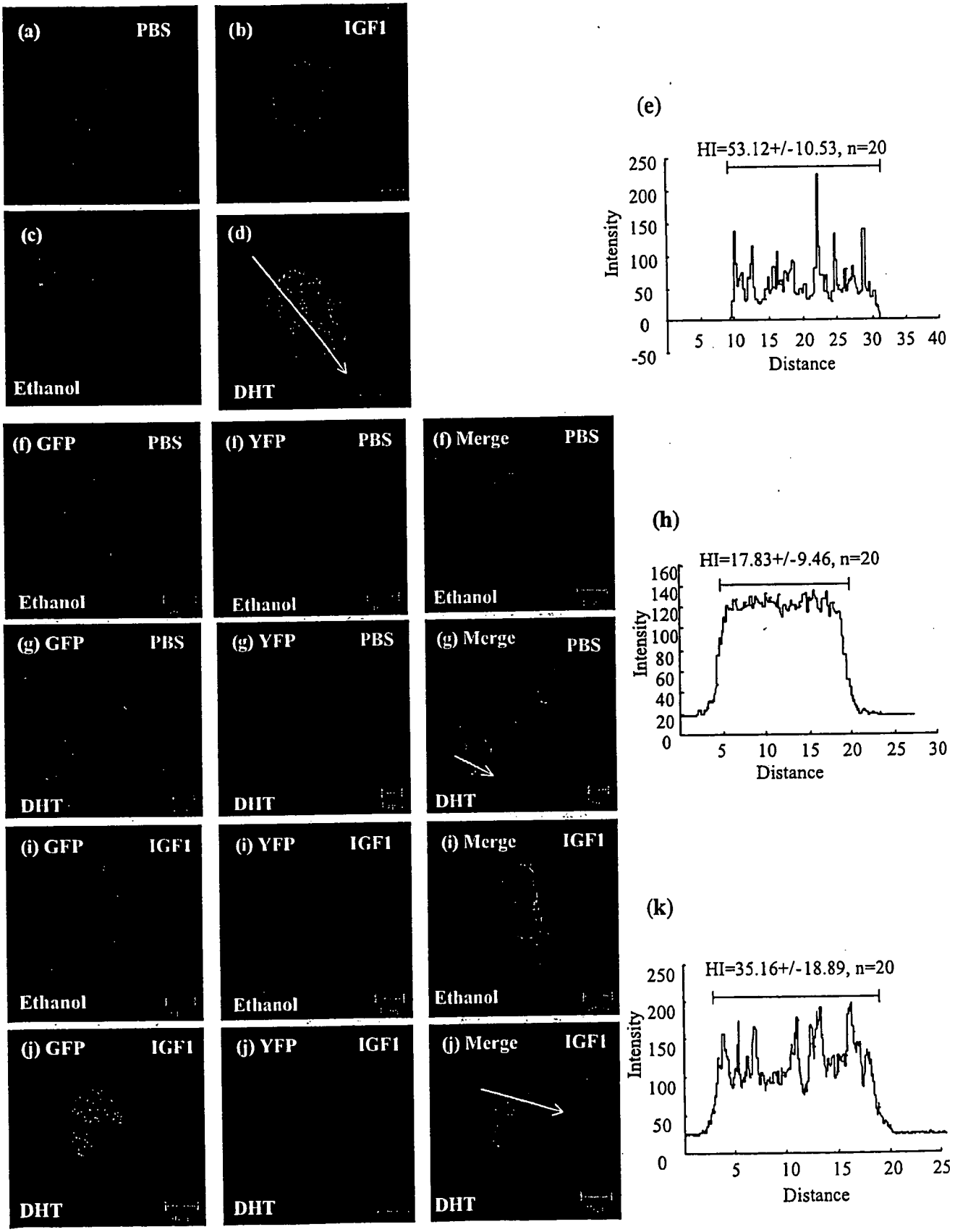
(a) PBS
(b) IGF1
(c) Ethanol
(d) DHT
(e)
HI=53.12+/-10.53, n=20
Intensity
Distance
(f) GFP PBS
(f) YFP PBS
(f) Merge PBS
Ethanol
(g) GFP PBS
(g) YFP PBS
(g) Merge PBS
DHT
(h)
HI=17.83+/-9.46, n=20
Intensity
Distance
(i) GFP IGF1
(i) YFP IGF1
(i) Merge IGF1
Ethanol
(j) GFP IGF1
(j) YFP IGF1
(j) Merge IGF1
DHT
(k)
HI=35.16+/-18.89, n=20
Intensity
Distance

Genomic DNA corresponding to the androgen-response elements ARE I/II and ARE III, which are located in the promoter and enhancer of the *PSA* gene, respectively, was remarkably enriched in a DHT-dependent manner, as evaluated using an anti-FLAG antibody (Fig. 5*b*). Weak bands were detectable in the absence of any ligand, whereas treatment of the cells with IGF1 or insulin either abolished or significantly reduced the occupancy of the DNA by Foxo1, regardless of the presence or absence of DHT. There was very weak Foxo1 occupancy of the DNA in a region between the enhancer and the promoter, but no enrichment was detected in the presence of DHT, thus demonstrating specificity (Fig. 5*b*). Again, the weak bands vanished in the presence of IGF1 or insulin. The association of Foxo1 with the chromatinized *PSA* promoter was specific, because DNA from the *GAPDH* gene was not precipitated (Fig. 5*b*). Thus, agonist-bound AR induces specific associations of Foxo1 with chromatin AREs on the *PSA* promoter, demonstrating that Foxo1 and AR form a ligand-dependent complex on chromatin. Furthermore, IGF1 and insulin are able to remove Foxo1 from chromatinized DNA.

The ChIP assays further revealed that Foxo1 interfered with ligand-induced recruitment of AR to the *PSA* promoter in LNCaP cells. The cells were transfected with pCMV-hAR together with pcDNA-FLAG-Foxo1-3A or pcDNA-FLAG and treated with the ligand as described above. Chromatin-transcription factor complexes were precipitated with an anti-AR antibody and combined with real time PCR analysis to quantify the relative number of immunoprecipitated DNA copies to the input control for each sample as described previously (24). Small amounts of the DNA segments corresponding to *PSA* ARE I/II and ARE III were detected in the absence of DHT, and DHT induced significant enrichment of these amounts (Fig. 5*c*). IGF1 or insulin increased the AR-DNA interaction under each circumstance (presence or absence of DHT; Fig. 5*c*). Overexpression of the nonphosphorylatable Foxo1-3A significantly reduced the relative copy numbers of *PSA* promoter DNA at both positions, especially in the presence of DHT (Fig. 5*c*), suggesting that the association between the *PSA* promoter and liganded AR was impaired. Furthermore, Foxo1-3A also substantially abolished the responsiveness to IGF1 and insulin (Fig. 5*c*), indicating that intact and phosphorylatable Foxo1 is vital for IGF1 or insulin to enhance the liganded AR-DNA interaction.

Activation of AR Stimulates IGF1R Expression in LNCaP Cells—We further found that IGF1R expression was up-regulated in LNCaP cells in the presence of DHT. As shown in Fig. 6*a*, DHT treatment for 24 h dose-dependently increased the IGF1R mRNA levels in serum-starved LNCaP cells, and 10^{-8} M DHT boosted the mRNA level by 17-fold. This stimulation of IGF1R was relatively specific, because comparable concentrations of DHT did not increase the levels of epidermal growth factor receptor (supplemental Fig. 9*a*) and Foxo1 mRNAs (supplemental Fig. 9*b*). An autoregulation process may occur, because the up-regulated IGF1R is expected to enhance IGF1-PI3K-Akt signaling, thereby resulting in a further gain-of-function of AR via phosphorylation of the repressive Foxo1.

DISCUSSION

Foxo1 Suppression and IGF1-related Mechanism of Refractory PC—IGF1 is capable of reactivating AR in low or absent androgen environments and therefore represents one of the suggested multiple mechanisms by which PC cells progress to the androgen-insensitive stage (7). However, the mechanisms by which IGF1 and other growth factors regulate AR-mediated transcription in PC cells remain unclear.

IGF1, via binding to its receptor IGF1R, activates intracellular signaling pathways that favor proliferation and cell survival. One of the most important pathways that becomes activated is the PI3K/Akt pathway (30), because activation of this pathway by IGF1, as well as other molecules, has been implicated in PC. Specifically, increases in IGF1R expression (11, 31, 32) and loss of the tumor suppressor gene *PTEN* (27, 28) elicit increased activity of the PI3K/Akt pathway and greatly contribute to tumor progression of PC.

Foxo1, which is endogenously expressed in PC cells, is functionally inhibited by phosphorylation at Ser-253, Ser-316, and Thr-(24 in response to IGF1 or insulin through PI3K/Akt kinase (17). Overexpression of Foxo1 in PC cells leads to apoptosis (33). Our present results have revealed that Foxo1 directly interacts with and suppresses the transactivation of AR, whereas IGF1 signaling ameliorates this suppression and results in AR gain-of-function. Thus, considering the reported mechanism that β-catenin may mediate the stimulatory effect of IGF1 signaling on AR (34), Foxo1 may represent an alternative explanation.

Because insulin induces PI3K-Akt signaling and the resultant modification of Foxo1 (17), similar to IGF1, and also enhances AR transactivation in PTEN-expressing LNCaP cells, it is of great value to further elucidate whether insulin signaling enhances AR function via a similar mechanism. Regarding this point, it is noteworthy that the syndrome of insulin resistance, which is characterized by an increased insulin level and abdom-

FIGURE 4. **Subcellular interaction between Foxo1 and AR in living COS7 cells.** The expressions of chimeric fluorescent proteins were observed in living COS7 cells using a Zeiss LSM 510 META laser confocal microscope as described under "Experimental Procedures." *a* and *b*, COS7 cells were transfected with 0.5 μg/dish of EYFP-Foxo1 and then treated with PBS (*a*) or 100 ng/ml IGF1 (*b*). *c* and *d*, COS7 cells expressing EGFP-AR were exposed to ethanol (*c*) or 10^{-8} M DHT (*d*), respectively. *f*, *g*, *i*, and *j*, COS7 cells coexpressing EGFP-AR and EYFP-Foxo1 were exposed to DHT and/or IGF1 as indicated in the individual panels. The fluorescence signals for green fluorescent protein (*GFP*) and yellow fluorescent protein (*YFP*) and the merged images are shown separately. *e*, *h*, and *k*, line scan analyses. A *straight line* was drawn through the target cell, and the fluorescence intensities along the line were recorded. The mean and S.D. values of the fluorescence intensity signals for the segment of interest (nucleus, avoiding the nucleoli) were calculated. The heterogeneity of the fluorescence intensity along the segment of interest was evaluated by the parameter of the HI, which was calculated using the following formula: HI = 100 × S.D./mean. A fluorescence intensity fluctuation graph, which clearly demonstrated the heterogeneity, was then created by plotting the intensity against the distance along the line. The lines obtained by line scan analyses are shown for representative cells. The fluorescence intensity fluctuation graphs of the representative cells are shown in *e*, *h*, and *k* and relate to the cells in *d*, *g*, and *j*, respectively. The *x* axis represents the distance along each line, whereas the *y* axis shows the fluorescence intensity. The *bar* within each graph marks the segment of the line for which the HI analysis was performed, and the corresponding intensity and HI values are indicated at the *top* of each graph. *Scale bars*, 10 μm.

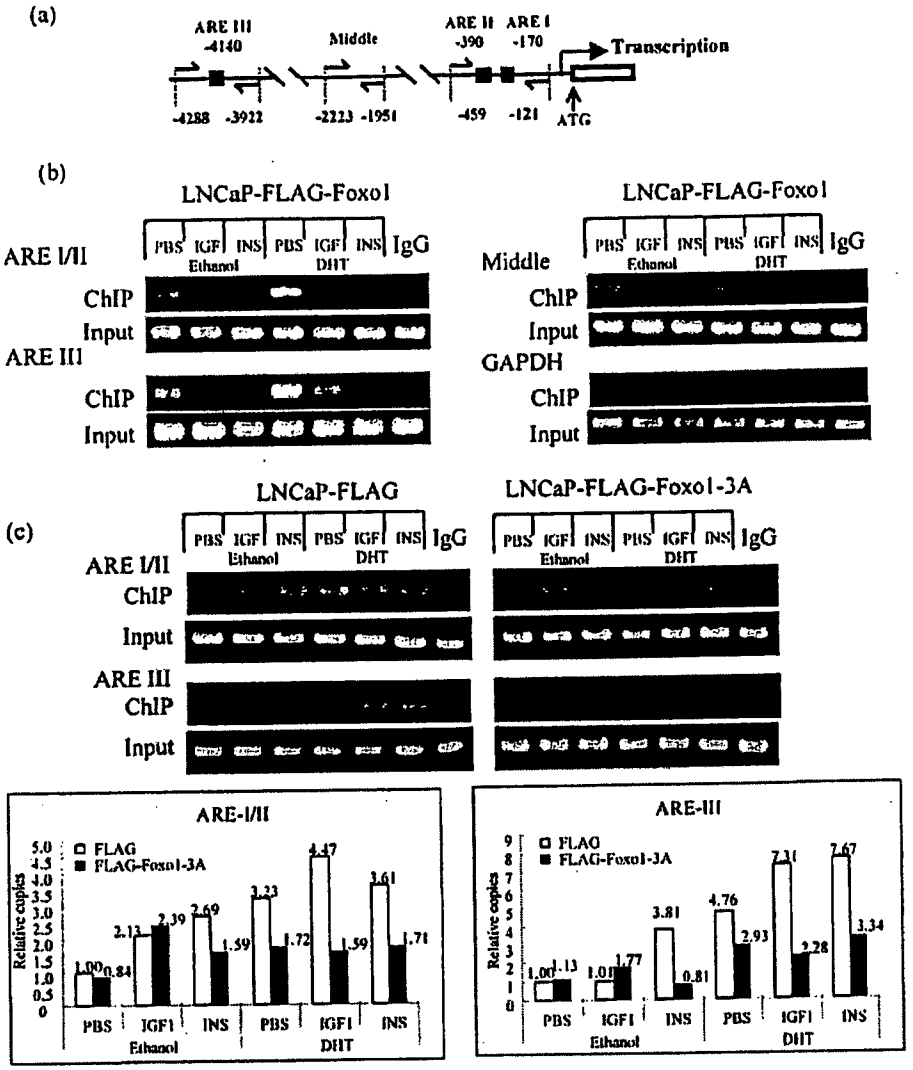

FIGURE 5. **Interaction of Foxo1 and AR within the human *PSA* promoter.** *a*, schematic diagram of the human *PSA* gene promoter region. The positions of the putative AREs are indicated, and the transcription start site is designated 1. *Pairs of arrows* indicate the PCR-amplified regions. *b*, occupancy of the *PSA* gene-regulatory regions by Foxo1. Soluble chromatin was prepared from FLAG-Foxo1-expressing LNCaP cells treated with the indicated ligands (10^{-8} M DHT; 100 ng/ml IGF1; 10 μg/ml insulin) for 30 min and then immunoprecipitated with an anti-FLAG antibody or normal mouse IgG as a control. Enrichment of ARE-containing DNA sequences in the immunoprecipitated DNA pool, indicating association of Foxo1 with the *PSA* promoter within intact chromatin, was visualized by PCR. The *lower panels* show the PCR-amplified *PSA* promoter bands from the input controls. *c*, effects of IGF1/insulin and Foxo1 on the occupancy of the *PSA* gene-regulatory regions by AR. Additional real time PCR was performed to quantify the amount of immunoprecipitated *PSA* promoter DNA copy numbers from cells under various treatments relative to their corresponding input controls.

inal obesity, is also associated with an increased incidence of PC and development of a more aggressive form of the disease (14, 15), although the mechanism remains unclear.

Nevertheless, the association between the risk of PC and the serum insulin level remains a controversial topic (35). There is even a lack of consensus over the association between the circulating level of IGF1 and the PC risk (30). With regard to this concern, our present results suggest that, in contrast to systemic circulating growth factors, there is also potential importance for the local bioavailability of growth factors and their cross-talk with hormones. Ligand-bound AR, which is functionally enhanced by IGF1-PI3K-Akt signaling-mediated dissociation of the repressor Foxo1, in turn stimulates the expression of IGF1R and presumably results in increased tension of IGF1 signaling, thereby leading to further functional augmentation of the receptor itself. Consistently, androgen withdrawal leads to a decrease in PI3K-Akt signaling (36, 37). Thus, as depicted in Fig. 6*b*, a mutually stimulatory feedback circuit (androgen-AR increases IGF1 signaling tension, whereas IGF1 signaling enhances AR transactivation), which works in an autocrine/intracrine manner in the local cellular environment of PC, may play important roles in up-regulation of AR function and PC progression.

AR Subnuclear Compartmentalization and Transactivation—Ligand-induced subnuclear compartmentalization (foci formation) is closely correlated with the transcriptional activation function of nuclear receptors (19–20, 22). DHT induces 250–400 fine and well separated subnuclear AR foci (19, 20), and the process is accompanied by the recruitment of coactivators such as SRC-1, TIF2, and CBP (20). AR bound to antiandrogens, such as hydroxyflutamide, does not form any foci (19), and cofactors that repress AR function readily disrupt DHT-induced foci formation by the receptor (18, 38). Our recent study further proved that the intranuclear complete/distinct foci formation of an agonist-bound steroid hormone receptor is an indicator of its transcriptional activation status (23).

Regarding this point, Foxo1 is able to disrupt AR nuclear translocation, and more importantly, the subnuclear foci formation induced by DHT is mechanistically significant. Although the mechanism remains to be elucidated, it can be speculated that Foxo1 may compete with coactivators, such as CBP, which is essential for AR foci formation (20) and for interaction with the receptor, and thereby inhibit the formation of transcriptionally active complexes. Importantly, our quantitative study revealed that IGF1 can rescue, at least partially, the Foxo1-disrupted AR subnuclear compartmentalization but not the disruption caused by the Akt-nonphosphorylatable constitutively active mutant Foxo1-3A. Therefore, Foxo1 interferes with the subnuclear compartmentalization of ligand-bound AR, and this effect is regulated by IGF1-PI3K-Akt signaling.

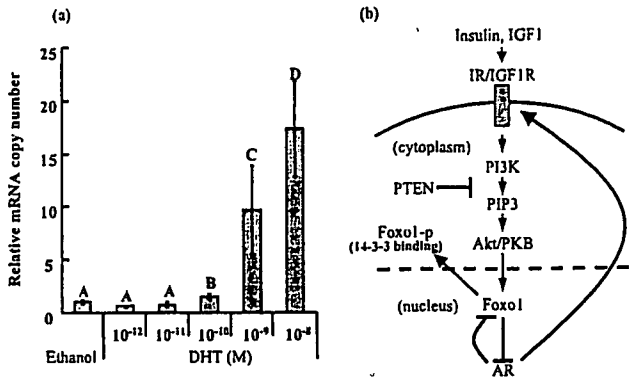

FIGURE 6. **Stimulatory feedback circuit between IGF1/insulin signaling and AR transactivation.** *a*, DHT up-regulates IGF1R mRNA expression. LNCaP cells were serum-starved and then incubated with increasing concentrations of DHT for 24 h. Next, total RNA was extracted and reverse-transcribed into cDNAs, before the IGF1R mRNA expression levels were analyzed by real time PCR as described under "Experimental Procedures." The relative mRNA amounts were normalized to the corresponding abundance of GAPDH mRNA. Triplicate results are expressed as the mean ± S.D. *Letters above the bars* show statistical groups (ANOVA, $p < 0.05$). *b*, proposed model for the cross-talk between IGF1/insulin signaling and AR. The local bioavailability of IGF1 (and/or insulin), which is probably abnormally high in PC, can be delivered from remote sites of production through the circulation or produced locally. Following ligand binding to IGF1R or insulin receptor, the tyrosine activity is activated, and this stimulates signaling pathways through intracellular networks that regulate cell proliferation and cell survival. One of the key downstream networks is the PI3K-Akt system. Akt, or a similar phosphatidylinositol 3,4,5-trisphosphate (*PIP3*)-dependent kinase, translocates to the nucleus and phosphorylates Ser-253, Ser-316, and Thr-24 of Foxo1. Phosphorylated Foxo1 is exported to the cytoplasm, where it has the potential to bind 14-3-3 protein and become retained in the cytoplasm. Foxo1 interacts with the C-terminal region of AR in the presence of a ligand (androgens such as DHT) and interferes with the ligand-induced subnuclear compartmentalization of AR, as well as the liganded receptor-target gene promoter interaction, thereby shutting down the AR transactivation. Modification of Foxo1 by the PI3K-Akt system, which is activated by IGF1 and/or insulin, weakens the Foxo1-AR interaction and ameliorates the inhibitory effects of Foxo1 on AR. Ligand-bound AR, in turn, stimulates the expression of IGF1R, resulting in enhanced IGF1 signaling tension. Moreover, liganded AR may also strengthen the net outcome of the IGF1-PI3K-Akt-Foxo1 axis by inducing biodegradation and/or direct functional inhibition of Foxo1, which results in further amelioration of Foxo1-related apoptosis of PC cells. These mutually inhibitory interactions between AR and Foxo1 functioning in the context of a positive feedback circuit between AR and IGF1 signaling and working in an autocrine/intracrine manner in the local cellular environment may play important roles in AR function modulation, prostate cell apoptosis, and also PC etiology and progression.

Foxo1-AR Interaction and Its Structural Basis and Regulation—The direct interaction between Foxo1 and AR is ligand (DHT)-dependent and relies on the C terminus of the receptor, which is functionally ligand-dependent (20). Nuclear receptor cofactors bind to AR via peptide motifs called nuclear receptor boxes with a consensus sequence of LXXLL (L, leucine; *X*, any amino acid) (39). These boxes are present in the N terminus of Foxo1 and conserved from mice (^{459}LKELL^{463}) to humans (^{452}LKELL^{466}) (21). The role, if any, of this motif in mediating the Foxo1-AR interaction remains to be determined. The interaction is probably weakened, but not completely abolished, by IGF1, because IGF1 reduced the anti-AR antibody-immunoprecipitated Foxo1 levels and improved the Foxo1-disrupted AR subnuclear compartmentalization. Liganded AR also recruited Foxo1 to the chromatin of AR target gene promoters, where Foxo1, in turn, interfered with AR-DNA interactions, mirroring its disturbance of AR subnuclear compartmentalization. IGF1 or insulin, however, reduced the DNA occupancy by Foxo1 but consistently enhanced that by AR. These IGF1/insulin regulations probably rely on Akt-mediated phosphorylation of Foxo1, because the Foxo1-3A-inhibited AR-DNA interaction as well as the AR foci formation was not recovered by IGF1/insulin. Thus, IGF1, and perhaps also insulin, appears able to regulate the Foxo1-AR interaction via PI3K/Akt phosphorylation of Foxo1. It is important to note that the effects of IGF1 and insulin on AR function are similar but not identical. IGF1 is generally more potent and efficient at enhancing AR transactivation, ameliorating the DHT-induced Foxo1-AR interaction and rescuing the Foxo1-interupted AR subnuclear compartmentalization (data not shown), although the difference was not that obvious in the ChIP assays. This phenomenon is presumably because of differential phosphorylation patterns of Foxo1 in response to IGF1 and insulin signaling. Although both hormones bind to their cognate receptors and activate the PI3K-Akt kinase cascade, which phosphorylates Foxo1 at Thr-24, Ser-253, and Ser-316, previous studies on hepatocytes (17) revealed that the phosphorylation patterns differ. Although the signaling pathways triggered by IGF1R and insulin receptor both phosphorylate the Akt site at Ser-253, which is a prerequisite for phosphorylation of the other two potential Akt sites Thr-24 and Ser-316, Thr-24 is phosphorylated by an unknown kinase that is specifically induced by insulin receptor. This type of site-specific phosphorylation of Foxo1, and the corresponding profiles of kinases downstream of IGF1 and insulin receptor in the LNCaP cellular environment, may provide a potential explanation for the different effects of IGF1 and insulin on the Foxo1-AR interaction as well as AR function.

It is noteworthy that another group also investigated the Foxo1-AR interaction recently (40). Consistent with our data, full-length AR, as well as its C-terminal ligand-binding domain, was found to interact with Foxo1 in an androgen-dependent manner, although the authors also reported a ligand-independent interaction between the N-terminal A/B region of the receptor and Foxo1, which we did not observe in our mammalian two-hybrid assays. Through direct interactions, ligand-bound AR was found to be able to inhibit DNA binding, as well as the transactivation activity of Foxo1, and impair the ability of Foxo1 to induce prostate cell apoptosis and cell cycle arrest (40). Liganded AR is also reportedly able to induce Foxo1 protein proteolysis and therefore ameliorate Foxo1-related apoptosis of PC cells (41). These studies, in combination with our present findings, suggest that AR and Foxo1 are mutually suppressive in terms of functional regulation. Besides the above-mentioned IGF1R up-regulation, inhibition of Foxo1 provides an additional way in which liganded AR may enhance the IGF1/insulin-PI3K-Akt-Foxo1 axis. The mutual inhibition between Foxo1 and AR in the context of IGF1 signaling may play an important role in AR function and prostate cell apoptosis, as well as in PC etiology and progression (Fig. 6*b*).

Taken together, the present results have identified Foxo1, a molecule functionally inhibited by IGF1/insulin-PI3K-Akt signaling, as a novel corepressor for AR. The results further suggest that positive feedback between the growth factor and androgen in the local cellular environment may play important roles in the regulation of AR transactivation. These findings provide a new mechanism by which IGF1, and also potentially

insulin, enhances AR transactivation and may shed new light on our understanding of the progression of PC to the androgen-insensitive stage. Pharmacological strategies that reduce IGF1/insulin signaling, in combination with antiandrogen therapies, are expected to have clinical benefits in fighting PC.

REFERENCES

1. Brinkmann, A. O., and Trapman, J. (2004) *Adv. Pharmacol.* **47**, 317–341
2. Greenlee, R. T., Murray, T., Bolden, S., and Wingo, P. A. (2000) *CA-Cancer. J. Clin.* **50**, 7–33
3. Santos, A. F., Huang, H., and Tindall, D. J. (2004) *Steroids* **69**, 79–85
4. Zegarra-Moro, O. L., Schmidt, L. J., Huang, H., and Tindall, D. J. (2002) *Cancer Res.* **62**, 1008–1013
5. Chen, C. D., Welsbie, D. S., Tran, C., Baek, S. H., Chen, R., Vessella, R., Rosenfeld, M. G., and Sawyers, C. L. (2004) *Nat. Med.* **10**, 33–39
6. Buchanan, G., Irvine, R. A., Coetzee, G. A., and Tilley, W. D. (2001) *Cancer Metastasis Rev.* **20**, 207–223
7. Grossmann, M. E., Huang, H., and Tindall, D. J. (2001) *J. Natl. Cancer. Inst.* **93**, 1687–1697
8. Pollak, M., Beamer, W., and Zhang, J. C. (1998) *Cancer Metastasis Rev.* **17**, 383–390
9. Wolk, A., Mantzoros, C. S., Andersson, S. O., Bergstrom, R., Signorello, L. B., Lagiou, P., Adami, H. O., and Trichopoulos, D. (1998) *J. Natl. Cancer. Inst.* **90**, 911–915
10. Burfeind, P., Chernicky, C. L., Rininsland, F., and Ilan, J. (1996) *Proc. Natl. Acad. Sci. U. S. A.* **93**, 7263–7268
11. Nickerson, T., Chang, F., Lorimer, D., Smeekens, S. P., Sawyers, C. L., and Pollak, M. (2001) *Cancer Res.* **61**, 6276–6280
12. Culig, Z., Hobisch, A., Cronauer, M. V., Radmayr, C., Trapman, J., Hittmair, A., Bartsch, G., and Klocker, H. (1994) *Cancer Res.* **54**, 5474–5478
13. Orio, F., Jr., Terouanne, B., Georget, V., Lumbroso, S., Avances, C., Siatka, C., and Sultan, C. (2002) *Mol. Cell. Endocrinol.* **198**, 105–114
14. Amling, C. L. (2005) *Curr. Opin. Urol.* **15**, 167–171
15. Hsing, A. W., Gao, Y. T., Chua, S., Jr., Deng, J., and Stanczyk, F. Z. (2003) *J. Natl. Cancer Inst.* **95**, 67–71
16. Kops, G. J., and Burgering, B. M. (1999) *J. Mol. Med.* **77**, 656–665
17. Nakae, J., Barr, V., and Accili, D. (2000) *EMBO J.* **19**, 989–996
18. Chen, G., Nomura, M., Morinaga, H., Matsubara, E., Okabe, T., Goto, K., Yanase, T., Zheng, H., Lu, J., and Nawata, H. (2005) *J. Biol. Chem.* **280**, 36355–36363
19. Tomura, A., Goto, K., Morinaga, H., Nomura, M., Okabe, T., Yanase, T., Takayanagi, R., and Nawata, H. (2001) *J. Biol. Chem.* **276**, 28395–28401
20. Saitoh, M., Takayanagi, R., Goto, K., Fukamizu, A., Tomura, A., Yanase, T., and Nawata, H. (2002) *Mol. Endocrinol.* **16**, 694–706
21. Nakae, J., Cao, Y., Daitoku, H., Fukamizu, A., Ogawa, W., Yano, Y., and Hayashi, Y. (2006) *J. Clin. Investig.* **116**, 2473–2483
22. Fan, W., Yanase, T., Wu, Y., Kawate, H., Saitoh, M., Oba, K., Nomura, M., Okabe, T., Goto, K., Yanagisawa, J., Kato, S., Takayanagi, R., and Nawata, H. (2004) *Mol. Endocrinol.* **18**, 127–141
23. Wu, Y., Kawate, H., Ohnaka, K., Nawata, H., and Takayanagi, R. (2006) *Mol. Cell. Biol.* **26**, 6633–6655
24. Fan, W., Yanase, T., Morinaga, H., Mu, Y. M., Nomura, M., Okabe, T., Goto, K., Harada, N., and Nawata, H. (2005) *Endocrinology* **146**, 85–92
25. Fan, W., Yanase, T., Nomura, M., Okabe, T., Goto, K., Sato, T., Kawano, H., Kato, S., and Nawata, H. (2005) *Diabetes* **54**, 1000–1008
26. Pfaffl, M. W. (2001) *Nucleic Acids Res.* **29**, e45
27. Xin, L., Teitell, M. A., Lawson, D. A., Kwon, A., Mellinghoff, I. K., and Witte, O. N. (2006) *Proc. Natl. Acad. Sci. U. S. A.* **103**, 7789–7794
28. McMenamin, M. E., Soung, P., Perera, S., Kaplan, I., Loda, M., and Sellers, W. R. (1999) *Cancer Res.* **59**, 4291–4296
29. Liao, G., Chen, L. Y., Zhang, A., Godavarthy, A., Xia, F., Ghosh, J. C., Li, H., and Chen, J. D. (2003) *J. Biol. Chem.* **278**, 5052–5061
30. Pollak, M. N., Schernhammer, E. S., and Hankinson, S. E. (2004) *Nat. Rev. Cancer* **4**, 505–518
31. Hellawell, G. O., Turner, G. D., Davies, D. R., Poulsom, R., Brewster, S. F., and Macaulay, V. M. (2002) *Cancer Res.* **62**, 2942–2950
32. Grzmil, M., Hemmerlein, B., Thelen, P., Schweyer, S., and Burfeind, P. (2004) *J. Pathol.* **202**, 50–59
33. Modur, V., Nagarajan, R., Evers, B. M., and Milbrandt, J. (2002) *J. Biol. Chem.* **277**, 47928–47937
34. Verras, M., and Sun, Z. (2005) *Mol. Endocrinol.* **19**, 391–398
35. Stattin, P., and Kaaks, R. (2003) *J. Natl. Cancer Inst.* **95**, 1086–1087
36. Baron, S., Manin, M., Beaudoin, C., Leotoing, L., Communal, Y., Veyssiere, G., and Morel, L. (2004) *J. Biol. Chem.* **279**, 14579–14586
37. Castoria, G., Lombardi, M., Barone, M. V., Bilancio, A., Di Domenico, M., De Falco, A., Varricchio, L., Bottero, D., Nanayakkara, M., Migliaccio, A., and Auricchio, F. (2004) *Steroids* **69**, 517–522
38. Tao, R. H., Kawate, H., Wu, Y., Ohnaka, K., Ishizuka, M., Inoue, A., Hagiwara, H., and Takayanagi, R. (2006) *Mol. Cell. Endocrinol.* **247**, 150–165
39. McInerney, E. M., Rose, D. W., Flynn, S. E., Westin, S., Mullen, T. M., Krones, A., Inostroza, J., Torchia, J., Nolte, R. T., Assa-Munt, N., Milburn, M. V., Glass, C. K., and Rosenfeld, M. G. (1998) *Genes Dev.* **12**, 3357–3368
40. Li, P., Lee, H., Guo, S., Unterman, T. G., Jenster, G., and Bai, W. (2003) *Mol. Cell. Biol.* **23**, 104–118
41. Huang, H., Muddiman, D. C., and Tindall, D. J. (2004) *J. Biol. Chem.* **279**, 13866–13877

Endocrine Journal 2007, 54 (1), 153–162

NOTE

Changes in Serum Sex Hormone Profiles after Short-term Low-dose Administration of Dehydroepiandrosterone (DHEA) to Young and Elderly Persons

YOSHIHIKO YAMADA, HISAHIKO SEKIHARA, MASAO OMURA, TOSHIHIKO YANASE*, RYOICHI TAKAYANAGI**, TOMOATSU MUNE***, KEIGO YASUDA***, TATSUO ISHIZUKA#, HAJIME UESHIBA##, YUKITAKA MIYACHI##†, TOMOYUKI IWASAKI, ATSUSHI NAKAJIMA### AND HAJIME NAWATA*

Department of Endocrinology and Metabolism, Yokohama City University Graduate School of Medicine
**Department of Medicine and Bioregulatory Science, Graduate School of Medical Sciences, Kyushu University*
***Department of Geriatric Medicine, Graduate School of Medical Sciences, Kyushu University*
****Department of Endocrinology, Diabetes and Rheumatology, Gifu University School of Medicine*
#General Internal Medicine, Gifu University School of Medicine
##First Department of Internal Medicine, Toho University School of Medicine
###Department of Gastroenterology, Yokohama City University Graduate School of Medicine

Abstract. In man, serum concentrations of dehydroepiandrosterone (DHEA) and DHEA sulfate (DHEAS) decrease with age after the twenties. For this reason, the decline in DHEA and DHEAS concentrations may be related to the development of some chronic diseases that are prevalent in the older age population. In this study, we evaluate the benefit and safety level of DHEA administration to men as a hormone replacement therapy. Twenty-two healthy Japanese males (age 26–63; mean ± SD, 41.0 ± 10.0 yrs.) received 25 mg DHEA once a day orally in the morning for two weeks. Serum concentrations of steroid hormones and cytokines were measured before and after the DHEA administration. Glucose tolerance and insulin resistance were also assessed before and after the DHEA administration using a 75 g oral glucose tolerance test and homeostasis model assessment (HOMA-R), respectively. Serum DHEA and DHEAS levels were significantly elevated after the DHEA administration for all ages of test subjects. In subjects who were older than 41 yrs. (older group) serum androstenedione and estradiol levels were elevated after the DHEA administration. Significant negative correlations were observed between the serum DHEA concentration and the serum concentration of fasting insulin, HOMA-R, leptin, and high-sensitivity C-reactive protein for all subjects. Daily administration of 25 mg DHEA increased the serum DHEA, DHEAS, androstenedione, and estradiol levels of the subjects of the older group to the same level as that of younger subjects.

Key words: Dehydroepiandrosterone (DHEA), Dehydroepiandrosterone sulfate (DHEAS), Androgen, Hormone replacement, Insulin resistance

(*Endocrine Journal* 54: 153–162, 2007)

WHILE it is known that there is an abundance of dehydroepiandrosterone (DHEA) and its sulfate conjugate (DHEAS) in the peripheral circulation in humans, their essential physiological roles still remain unclear. It is known that the secretion of DHEA increases with postnatal aging peaking in the twenties, and then decreases with age afterwards. Due to this type of dynamic change, the decline in DHEA and DHEAS secretion based on aging is compared to female menopause and expressed as adrenopause. The relationship of DHEA and DHEAS to symptoms of senility and geriatric disease has attracted much attention [1]. The re-

Received: September 26, 2005
Accepted: October 4, 2006
Correspondence to: Dr. Yoshihiko YAMADA, Department of Internal Medicine, Atami Hospital, International University of Health and Welfare, 13-1 Higashikaigan-cho, Atami, Shizuoka 413-0012, Japan
† Dr. Yukitaka Miyachi passed away on January 23, 2003.

port by Roth [2] shows that the lifespan of a person and the serum concentration of DHEA are related. There are also reports related to antiatherosclerotic [3–6], antidiabetic [7–9], antiinflammatory [10–12], and anti-osteoporotic functions [13, 14], and we anticipate that DHEA has the so-called antisenility hormone function related to the aging phenomenon.

Hormone replacement therapy is a method for preventing or treating various chronic diseases associated with aging by replacing sex steroid hormones the levels of which decrease due to aging. In aging societies of various advanced countries, concern is on the rise regarding hormone replacement therapy. Although there are many studies underway on estrogen replacement therapy for postmenopausal women [15–18], the number of such studies on male hormone replacement therapy is not at the same level. In particular, there are only a few studies on the Japanese population [19, 20]. We conducted an investigation on a short-term and low-dose replacement therapy with DHEA on Japanese men and studied the influence on hormone dynamics, glucose tolerance, and insulin resistance.

Materials and Methods

Test subjects

Twenty-two normal healthy Japanese males (age 26–63; mean ± SD, 41.0 ± 10.0 yrs.) volunteered to be test subjects. Baseline characteristics of the 22 subjects are outlined in Table 1.

Test design

An open-label test format was used. All subjects received 25 mg DHEA once a day orally in the morning for two weeks. The DHEA is a product of Advanced Brain Research Foundation, Inc. (Cambridge, MA) and was purchased from Gloria International Inc. (Tokyo, Japan). Blood sampling and a 75 g oral glucose tolerance test (75 g OGTT) were performed after 12 h of fasting on the day before and then after two weeks of the DHEA administration. Approval for this study was obtained from the Yokohama City University Hospital Ethical Committee.

Measurement

Serum DHEA, DHEAS, androstenedione, estradiol

Table 1. Baseline Characteristics of 22 Subjects

Age (yr)	BMI (kg/m²)	FPG (mmol/l)	F-insulin (pmol/l)	HOMA-R	DHEA (nmol/l)	DHEAS (μmol/l)
63	23.3	6.2	159	7.26	11.1	2.5
41	24.1	5.6	29	1.18	26.7	5.6
49	23.0	5.2	27	1.02	12.8	3.2
40	24.1	5.4	61	2.44	9.0	5.2
35	22.8	5.7	169	7.15	6.6	5.0
35	23.9	4.5	35	1.17	18.7	3.4
30	21.9	5.5	57	2.32	26.7	15.6
27	18.9	5.2	84	3.25	24.6	13.0
30	33.1	5.8	134	5.78	8.7	11.3
44	21.2	4.9	23	0.82	10.4	3.0
51	24.8	6.6	60	2.91	20.5	5.5
43	22.9	5.2	42	1.60	22.9	7.6
46	22.0	5.4	32	1.27	20.8	12.0
31	20.0	5.8	35	1.51	55.5	8.0
26	21.0	5.1	35	1.33	11.8	6.2
26	27.3	5.5	41	1.66	23.9	7.4
49	22.9	5.5	45	1.85	9.0	3.1
49	21.5	5.1	74	2.79	28.8	4.3
42	23.0	5.2	19	0.71	17.7	7.2
51	21.8	5.0	25	0.97	34.3	9.1
51	22.9	5.0	37	1.38	15.3	8.7
43	20.4	4.4	58	1.89	31.2	12.6

BMI: Body mass index, FPG: Fasting plasma glucose, F-insulin: Fasting serum insulin

(E2), and free testosterone were measured using the solid phase radioimmunoassay (Diagnostic Products Corporation, CA, USA). Serum IGF-1 was measured using the solid phase radioimmunoassay (Daiichi Radioisotope Corporation, Tokyo, Japan). All of these measurements and complete blood count, liver function, renal function, electrolytes, lipids, glucose, and insulin measurements were performed in commercial laboratories (SRL, Inc., Tokyo, Japan).

Evaluation of insulin resistance was assessed with homeostasis model assessment (HOMA-R) and calculated using the following formula: fasting plasma glucose (mmol/L) × fasting serum insulin (micro U/mL) divided by 25 [21]. We calculated the insulinogenic index, as the initial insulin secretion response index after glucose tolerance, using a previously described method [22, 23].

The serum concentration of leptin, adiponectin, and high-sensitivity C-reactive protein (hsCRP) was measured by radioimmunoassay (Cosmic Corporation, Tokyo, Japan), ELISA (Otsuka Pharmaceutical Co. Ltd., Tokyo, Japan), and nephelometry (Dade Behring Inc., IL, USA), respectively. The plasma concentration of soluble intercellular adhesion molecule-1 (ICAM-1), soluble vascular cell adhesion molecule-1 (VCAM-1), and tumor necrosis factor alpha (TNF alpha) was measured by EIA (Bender Medsystems, Vienna, Austria), EIA (R&D Systems Inc., MN, USA), and ELISA (Japan Immunoresearch Laboratories Co. Ltd., Gunma, Japan), respectively.

Statistical analysis

Statistical analysis was performed using StatView 5.0 for Windows®. Paired t test, two-sample t independent-group test, the Wilcoxon signed-rank test, and the Mann Whitney U test were used to compare each of the measured values of the basic level before the administration of DHEA and that after two weeks of administration. The Spearman ranking correlation coefficient was used to verify the correlation coefficient. A P value <0.05 was considered statistically significant.

Results

Change in hormone concentration in blood

Table 2 gives the hormone concentration before and after the DHEA administration. After administration of 25 mg DHEA for two weeks, the serum concentration of DHEA, DHEAS, and androstenedione exhibited a significant increase; however, IGF-1, E2, and testosterone showed no significant change. Because the basal level of the serum DHEA and DHEAS concentration decreases with age, subjects were divided into two groups according to their age. The subjects who were ≤41 years of age were classified into the younger group, and those >41 years of age were classified into the older group. In the younger group, after two week administration of 25 mg DHEA, the serum concentration of DHEA and DHEAS exhibited a significant increase. In the older group, after two week administration of 25 mg DHEA, in addition to DHEA and DHEAS, the concentration of androstenedione and E2 exhibited a significant increase. For comparison of dosage effectiveness, we tested the administration of 50 mg DHEA as a preliminary study. Table 2 also gives the hormone concentration after the 50 mg DHEA administration. There were no differences in

Table 2.

Age (yr)	25 mg DHEA administered						50 mg DHEA administered (n = 6) 51.8 ± 7.5	
	All (n = 22) 41.1 ± 10.0		Younger (n = 10) 32.1 ± 5.5		Older (n = 12) 48.4 ± 5.7			
	Baseline	2 weeks	Baseline	2 weeks	Baseline	2 weeks	Baseline	2 weeks
DHEA (nmol/l)	20.3 ± 11.3	29.6 ± 15.9[d]	21.2 ± 14.4	27.1 ± 15.0[a]	19.6 ± 8.5	31.8 ± 16.9[b]	21.0 ± 5.3	33.1 ± 16.7
DHEAS (μmol/l)	7.3 ± 3.7	12.0 ± 4.0[f]	8.1 ± 3.9	12.4 ± 2.8[e]	6.6 ± 3.5	11.7 ± 5.0[e]	5.3 ± 2.3	11.9 ± 4.2[b]
Androstenedione (nmol/l)	7.9 ± 2.2	10.7 ± 2.7[e]	8.3 ± 3.0	10.3 ± 3.1	7.6 ± 1.3	11.1 ± 2.4[e]	6.8 ± 2.9	12.2 ± 4.5[a]
Estradiol (pmol/l)	112 ± 50	118 ± 34	126 ± 64	106 ± 31	100 ± 34	127 ± 34[a]	67 ± 25	85 ± 9
Testosterone (nmol/l)	16.6 ± 4.2	16.4 ± 4.5	17.0 ± 5.8	16.7 ± 5.6	16.3 ± 2.4	16.2 ± 3.7	12.9 ± 5.7	13.0 ± 3.5
IGF-1 (nmol/l)	24.9 ± 6.7	26.2 ± 7.7	28.7 ± 6.8	28.6 ± 6.6	21.7 ± 5.0	24.2 ± 8.3	22.5 ± 8.8	24.9 ± 6.6

Values are expressed as the mean ± S.D. [a] $P<0.05$, [b] $P<0.01$, [c] $P<0.005$, [d] $P<0.001$, [e] $P<0.0005$, and [f] $P<0.0001$ compared with basal value

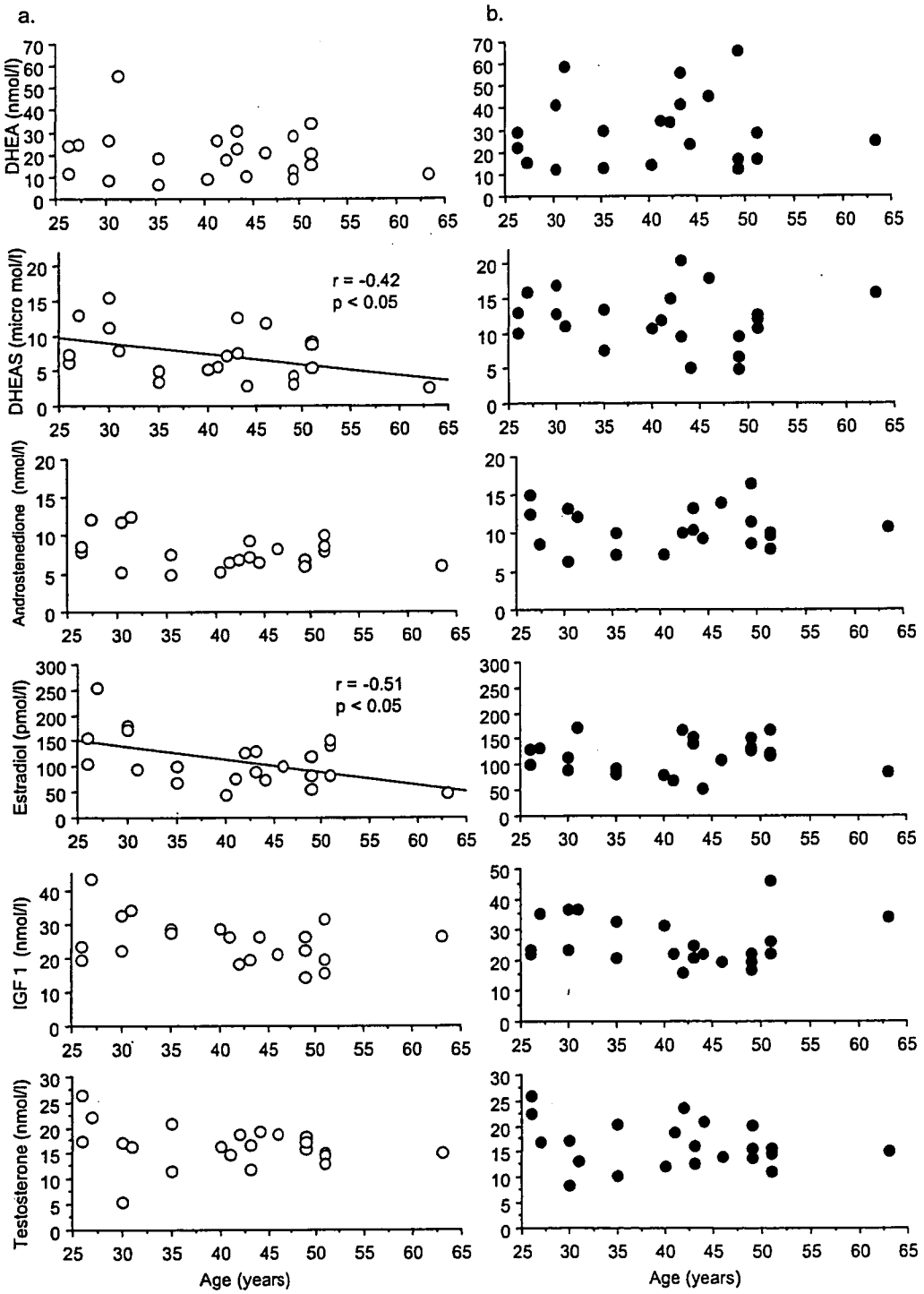

Fig. 1. Serum hormone levels before and after DHEA administration
a. Serum concentration of DHEA, DHEAS, androstenedione, estradiol, IGF-1, and testosterone before the DHEA administration (○). Serum concentration of DHEAS and estradiol was found to decrease significantly with age. b. Serum concentration of the same hormones after daily administration of 25 mg DHEA for two weeks (●). The decreases in DHEAS and E2 with age were no longer observed.

Table 3.

	All (n = 22)		Younger (n = 10)		Older (n = 12)	
	Baseline	2 weeks	Baseline	2 weeks	Baseline	2 weeks
Total cholesterol (mmol/l)	5.35 ± 1.18	5.29 ± 0.96	4.89 ± 1.11	5.66 ± 0.83	5.74 ± 1.14	5.65 ± 0.91
Triglyceride (mmol/l)	1.17 ± 0.68	0.95 ± 0.50	1.28 ± 0.67	1.00 ± 0.63	1.07 ± 0.70	0.92 ± 0.41
LDL cholesterol (mmol/l)	3.38 ± 1.02	3.24 ± 0.87	2.98 ± 0.97	2.90 ± 0.73	3.82 ± 0.94	3.61 ± 0.89
HDL cholesterol (mmol/l)	1.63 ± 0.43	1.64 ± 0.35	1.42 ± 0.25	1.48 ± 0.24	1.88 ± 0.47	1.82 ± 0.38

Values are expressed as the mean ± S.D.

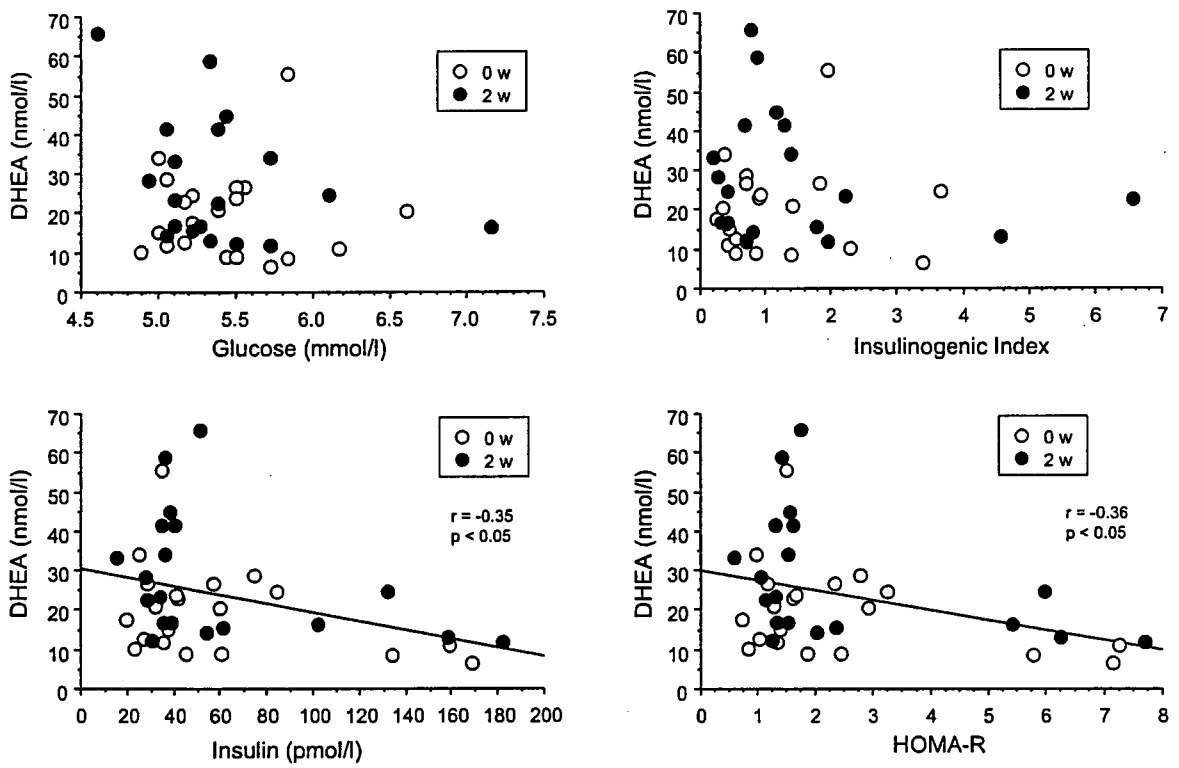

Fig. 2. Correlation between serum concentration of DHEA and glucose tolerance
Correlation of the serum level of DHEA with the fasting plasma glucose, fasting serum insulin, insulinogenic index, and HOMA-R before (○) and after (●) the DHEA administration. The fasting insulin titer and HOMA-R values correlated negatively with the serum level of DHEA.

any of the hormone concentrations between the 25 mg and 50 mg DHEA administration.

When investigating the correlation between age and each serum hormone concentration before and after the DHEA administration, serum DHEAS and E2 were found to decrease significantly with age. After the administration of 25 mg DHEA for two weeks, such age related decrease in DHEAS and E2 disappeared. Although there was a tendency for the serum concentration of DHEA and androstenedione to decrease with age, it was not statistically significant (Fig. 1). The serum hormone concentration of the older group was shown to increase to the same level as that of younger group for DHEA, DHEAS, androstenedione, and E2.

Effect on routine examination

After the administration of 25 mg DHEA for two weeks, there was no significant change in the complete blood count, liver function, renal function, electrolyte, or uric acid value (data not shown). In regard to the effect on lipids, there was no significant change in the

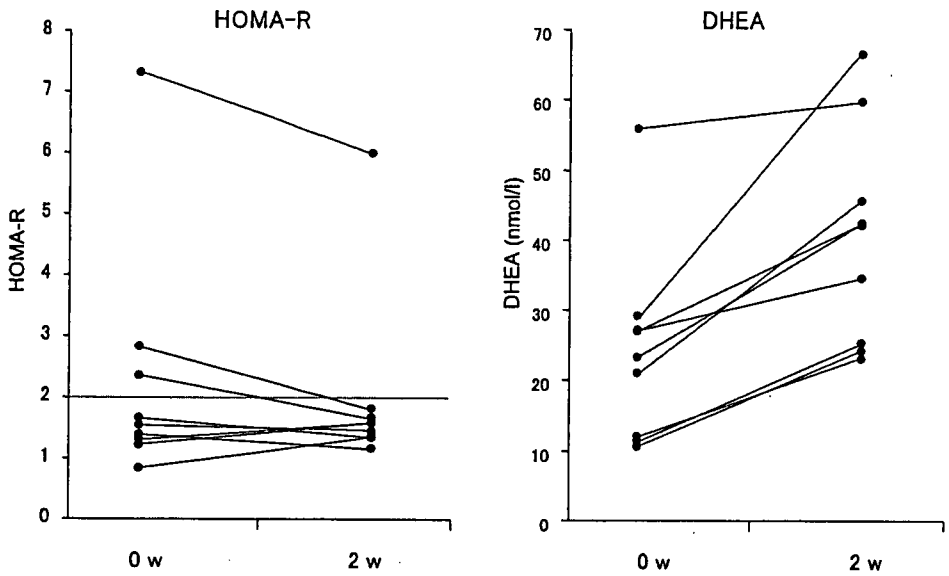

Fig. 3. Changes in HOMA-R among subjects whose serum DHEA level was elevated
In subjects with a HOMA-R higher than two, there is a clear decrease in the HOMA-R level after the two week DHEA administration.

total cholesterol, LDL cholesterol, HDL cholesterol, or triglyceride concentration as indicated in Table 3.

Effect on glucose metabolism

After the administration of 25 mg DHEA for two weeks, there was no significant change in the fasting plasma glucose and fasting serum insulin level. During 75 g OGTT, there were no significant changes in the two-hour plasma glucose level, HOMA-R, or insulinogenic index. However, when comparing the relationship between each evaluation item and the DHEA concentration, regardless of before or after administration, we recognized a significant negative correlation between the serum DHEA concentration and the fasting insulin concentration or the HOMA-R (Fig. 2). This finding indicates that the lower the blood DHEA level became, the higher the insulin resistance. In 19 subjects, HOMA-R was calculated before and after the two week administration of DHEA. There were nine subjects whose serum concentration of DHEA was elevated to higher than 21.1 nmol/l, which was the same as the mean concentration of the younger subjects. When a change in serum concentration of DHEA was compared to that for HOMA-R in each subject, three subjects with marked insulin resistance whose HOMA-R level was higher than 2.0 showed a decline in the HOMA-R level after 25 mg of DHEA administration as shown in Fig. 3. No constant tendency was observed in six normal insulin sensitivity subjects whose HOMA-R level was lower than 2.0. These findings suggest the possibility that when the serum concentration of DHEA exceeds a certain level as a result of hormone replacement therapy, insulin resistance reverts to normal (Fig. 3).

Correlation of serum DHEA concentration to cytokines and adhesion molecules (Before and after DHEA administration)

The relationship of the DHEA level to cytokines and adhesion molecules, which are thought to have a relationship with insulin resistance and atherosclerosis, were studied by determining leptin, adiponectin, hsCRP, TNF alpha, soluble ICAM-1, and soluble VCAM-1. There was a significant negative correlation between the serum DHEA concentration and the serum concentration of leptin and hsCRP as shown in Fig. 4. Furthermore, leptin exhibited a significant positive correlation with insulin, HOMA-R, and hsCRP, and a negative correlation with adiponectin as indicated in Fig. 5.

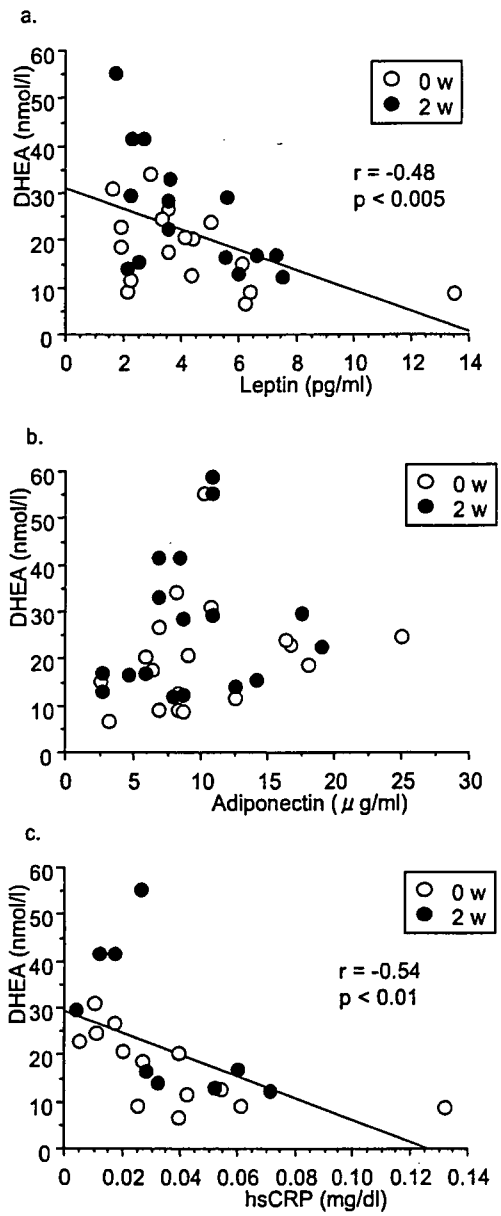

Fig. 4. Correlation of serum DHEA level with serum concentration of leptin, adiponectin and hsCRP before (○) and after (●) DHEA administration
The serum level of DHEA was found to correlate negatively with the serum concentration of leptin (a) and hsCRP (c).

Discussion

It is well known that the concentration of the male sex hormone decreases gradually with age, and discussion regarding the usefulness of hormone replacement therapy is becoming widespread [24–26]. Maintaining health and preventing chronic diseases in an aging society are important issues facing advanced countries, and DHEA replacement therapy is anticipated to be a possible solution to these problems. In this study, not only DHEA or DHEAS, but also androstenedione and E2 exhibited a tendency to decrease with age, and through the 25 mg per day DHEA administration the decreased levels of these hormone concentrations recovered to the same level as that of the younger subjects. In reports up to now, there have been many examples of replacement studies using doses greater than 50 mg per day [27–36]. However, in this study, we selected 25 mg per day of DHEA administration because the standard dose of many clinically available medicines for Western people tends to be equivalent to the maximum dose for Japanese. It is thought that the administration of a low dose of DHEA might be safer. According to the change in older group's hormone profiles, it is thought that even a 25 mg replacement regimen could be sufficient to obtain an increase in Japanese subjects. Further evaluation regarding the dose effectiveness is required.

In young subjects who exhibited a sufficiently high serum concentration of DHEA before the treatment, no significant change was observed after the 25 mg daily DHEA administration. This might be due to the extensive peripheral metabolism of the orally administered DHEA to other androgens and conjugates [37]. Together with the fact that there were no abnormal values from the blood test or biochemical examination, the above results support the notion that DHEA replacement therapy is safe [38]. However, since the administration was limited to a short two weeks in this study, future investigations are needed involving a low-dose long-term therapy and evaluation of the sex steroid hormone concentration in the blood and the side effects.

DHEA administration was reported to reduce visceral fat and to improve insulin resistance [39]. In the results of the 75 g OGTT administered this time, while there was no discernable influence on the plasma glucose level, we recognized the negative correlation between the serum DHEA concentration and the fasting insulin level or the HOMA-R. This is consistent with the previous report by Villareal and Holloszy [39].

In this investigation, we recognized that the serum DHEA concentration and the serum leptin concentration have a negative correlation, and this supports the

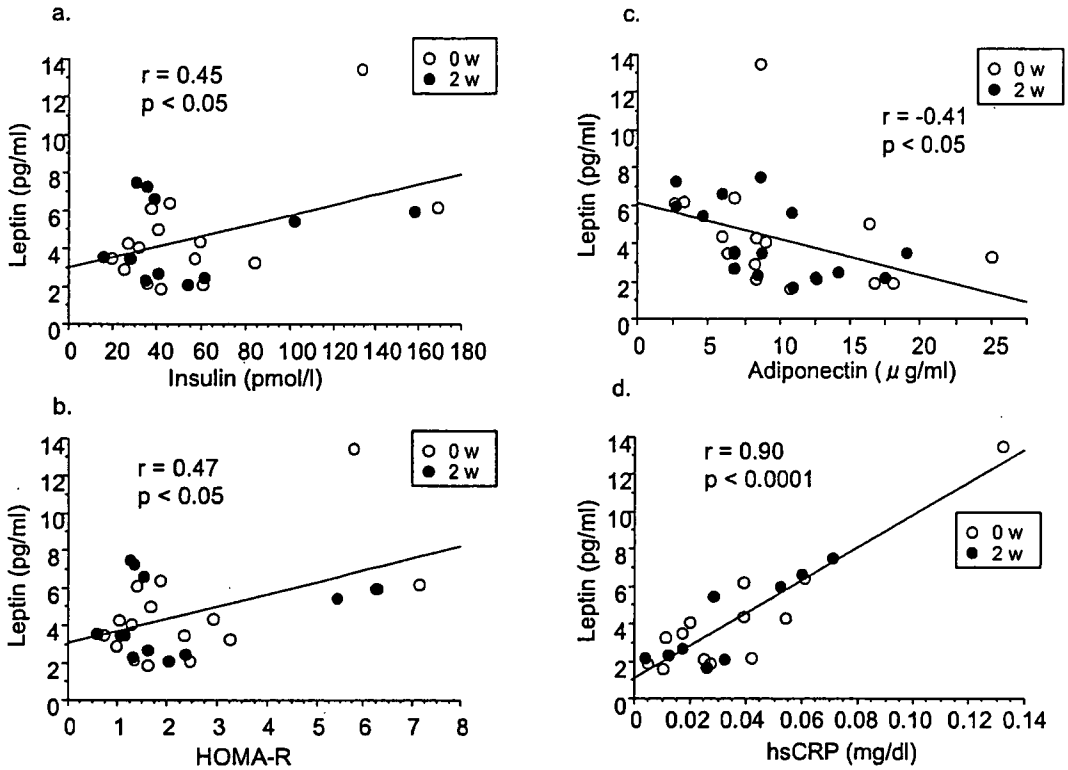

Fig. 5. Correlation of serum leptin level with insulin resistance and cytokines before (○) and after (●) DHEA administration Positive correlations were observed between the serum leptin level with insulin (a), HOMA-R (b) and hsCRP (d). Negative correlation was observed between the serum leptin level with adiponectin (c).

results reported by Callies *et al.* [30]. The significant positive correlation between the serum concentration of leptin and the insulin resistance were consistent with the findings of Segal *et al.* [40]. The relationship between the serum DHEA concentration and the onset frequency of myocardial infarction was identified in previous reports [6, 41]. The results of the current study indicating that there is a negative correlation between the serum DHEA concentration and hsCRP is consistent with the results reported by Leal *et al.* [42]. According to these results, the serum concentration of DHEA and various factors that are involved in insulin resistance might influence each other [43]. However, the mechanism for the correlation is not clear and further investigation is needed.

In conclusion, the results of this short-term low-dose DHEA administration regimen suggest that supplemental DHEA administration to healthy middle-aged and elderly male subjects may help maintain their serum sex steroid hormone concentration at a younger age level without appreciable side effects. The low dosage of DHEA replacement therapy is expected to have the effect of improving insulin resistance.

Acknowledgement

This study was supported by the Research Grant for Longevity Sciences (12C-03) from the Ministry of Health, Labour and Welfare, Japan.

References

1. Lamberts SW, van den Beld AW, van der Lely AJ (1997) The endocrinology of aging. *Science* 278: 419–424.
2. Roth GS, Lane MA, Ingram DK, Mattison JA, Elahi D,

Tobin JD, Muller D, Metter EJ (2002) Biomarkers of caloric restriction may predict longevity in humans. *Science* 297: 811.

3. Eich DM, Nestler JE, Johnson DE, Dworkin GH, Ko D, Wechsler AS, Hess ML (1993) Inhibition of accelerated coronary atherosclerosis with dehydroepiandrosterone in the heterotopic rabbit model of cardiac transplantation. *Circulation* 87: 261–269.
4. Gordon GB, Bush DE, Weisman HF (1988) Reduction of atherosclerosis by administration of dehydroepiandrosterone. A study in the hypercholesterolemic New Zealand white rabbit with aortic intimal injury. *J Clin Invest* 82: 712–720.
5. Herrington DM (1995) Dehydroepiandrosterone and coronary atherosclerosis. *Ann NY Acad Sci* 774: 271–280.
6. Herrington DM, Gordon GB, Achuff SC, Trejo JF, Weisman HF, Kwiterovich PO Jr, Pearson TA (1990) Plasma dehydroepiandrosterone and dehydroepiandrosterone sulfate in patients undergoing diagnostic coronary angiography. *J Am Coll Cardiol* 16: 862–870.
7. Aoki K, Saito T, Satoh S, Mukasa K, Kaneshiro M, Kawasaki S, Okamura A, Sekihara H (1999) Dehydroepiandrosterone suppresses the elevated hepatic glucose-6-phosphatase and fructose-1,6-bisphosphatase activities in C57BL/Ksj-db/db mice: comparison with troglitazone. *Diabetes* 48: 1579–1585.
8. Coleman DL, Leiter EH, Schwizer RW (1982) Therapeutic effects of dehydroepiandrosterone (DHEA) in diabetic mice. *Diabetes* 31:830–833.
9. Ladriere L, Laghmich A, Malaisse-Lagae F, Malaisse WJ (1997) Effect of dehydroepiandrosterone in hereditarily diabetic rats. *Cell Biochem Funct* 15: 287–292.
10. Du C, Khalil MW, Sriram S (2001) Administration of dehydroepiandrosterone suppresses experimental allergic encephalomyelitis in SJL/J mice. *J Immunol* 167: 7094–7101.
11. Straub RH, Konecna L, Hrach S, Rothe G, Kreutz M, Scholmerich J, Falk W, Lang B (1998) Serum dehydroepiandrosterone (DHEA) and DHEA sulfate are negatively correlated with serum interleukin-6 (IL-6), and DHEA inhibits IL-6 secretion from mononuclear cells in man in vitro: possible link between endocrinosenescence and immunosenescence. *J Clin Endocrinol Metab* 83: 2012–2017.
12. Yu CK, Yang BC, Lei HY, Chen YC, Liu YH, Chen CC, Liu CW (1999) Attenuation of house dust mite Dermatophagoides farinae-induced airway allergic responses in mice by dehydroepiandrosterone is correlated with down-regulation of TH2 response. *Clin Exp Allergy* 29: 414–422.
13. Kasperk CH, Wakley GK, Hierl T, Ziegler R (1997) Gonadal and adrenal androgens are potent regulators of human bone cell metabolism in vitro. *J Bone Miner Res* 12:464–471.
14. Labrie F, Diamond P, Cusan L, Gomez JL, Belanger A, Candas B (1997) Effect of 12-month dehydroepiandrosterone replacement therapy on bone, vagina, and endometrium in postmenopausal women. *J Clin Endocrinol Metab* 82: 3498–3505.
15. Anderson GL, Judd HL, Kaunitz AM, Barad DH, Beresford SA, Pettinger M, Liu J, McNeeley SG, Lopez AM (2003) Effects of estrogen plus progestin on gynecologic cancers and associated diagnostic procedures: the Women's Health Initiative randomized trial. *JAMA* 290: 1739–1748.
16. Cauley JA, Robbins J, Chen Z, Cummings SR, Jackson RD, LaCroix AZ, LeBoff M, Lewis CE, McGowan J, Neuner J, Pettinger M, Stefanick ML, Wactawski-Wende J, Watts NB (2003) Effects of estrogen plus progestin on risk of fracture and bone mineral density: the Women's Health Initiative randomized trial. *JAMA* 290: 1729–1738.
17. Harris RE, Chlebowski RT, Jackson RD, Frid DJ, Ascenseo JL, Anderson G, Loar A, Rodabough RJ, White E, McTiernan A (2003) Breast cancer and nonsteroidal anti-inflammatory drugs: prospective results from the Women's Health Initiative. *Cancer Res* 63: 6096–6101.
18. Rossouw JE, Anderson GL, Prentice RL, LaCroix AZ, Kooperberg C, Stefanick ML, Jackson RD, Beresford SA, Howard BV, Johnson KC, Kotchen JM, Ockene J (2002) Risks and benefits of estrogen plus progestin in healthy postmenopausal women: principal results From the Women's Health Initiative randomized controlled trial. *JAMA* 288: 321–333.
19. Kawano H, Yasue H, Kitagawa A, Hirai N, Yoshida T, Soejima H, Miyamoto S, Nakano M, Ogawa H (2003) Dehydroepiandrosterone supplementation improves endothelial function and insulin sensitivity in men. *J Clin Endocrinol Metab* 88: 3190–3195.
20. Sugino M, Ohsawa N, Ito T, Ishida S, Yamasaki H, Kimura F, Shinoda K (1998) A pilot study of dehydroepiandrosterone sulfate in myotonic dystrophy. *Neurology* 51: 586–589.
21. Matthews DR, Hosker JP, Rudenski AS, Naylor BA, Treacher DF, Turner RC (1985) Homeostasis model assessment: insulin resistance and beta-cell function from fasting plasma glucose and insulin concentrations in man. *Diabetologia* 28: 412–419.
22. Kosaka K, Kuzuya T, Hagura R, Yoshinaga H (1996) Insulin response to oral glucose load is consistently decreased in established non-insulin-dependent diabetes mellitus: the usefulness of decreased early insulin response as a predictor of non-insulin-dependent diabetes mellitus. *Diabet Med* 13: S109–119.
23. Seltzer HS, Allen EW, Herron AL Jr, Brennan MT (1967) Insulin secretion in response to glycemic stimulus: relation of delayed initial release to carbohydrate intolerance in mild diabetes mellitus. *J Clin Invest* 46:

323–335.
24. Demers LM (2003) Andropause: an androgen deficiency state in the ageing male. *Expert Opin Pharmacother* 4: 183–190.
25. Tenover JS (1998) Androgen replacement therapy to reverse and/or prevent age-associated sarcopenia in men. *Baillieres Clin Endocrinol Metab* 12: 419–425.
26. Vermeulen A (2000) Andropause. *Maturitas* 34: 5–15.
27. Achermann JC, Silverman BL (2001) Dehydroepiandrosterone replacement for patients with adrenal insufficiency. *Lancet* 357: 1381–1382.
28. Arlt W (2002) Quality of life in Addison's disease — the case for DHEA replacement. *Clin Endocrinol (Oxf)* 56: 573–574.
29. Arlt W, Callies F, van Vlijmen JC, Koehler I, Reincke M, Bidlingmaier M, Huebler D, Oettel M, Ernst M, Schulte HM, Allolio B (1999) Dehydroepiandrosterone replacement in women with adrenal insufficiency. *N Engl J Med* 341: 1013–1020.
30. Callies F, Fassnacht M, van Vlijmen JC, Koehler I, Huebler D, Seibel MJ, Arlt W, Allolio B (2001) Dehydroepiandrosterone replacement in women with adrenal insufficiency: effects on body composition, serum leptin, bone turnover, and exercise capacity. *J Clin Endocrinol Metab* 86: 1968–1972.
31. Gebre-Medhin G, Husebye ES, Mallmin H, Helstrom L, Berne C, Karlsson FA, Kampe O (2000) Oral dehydroepiandrosterone (DHEA) replacement therapy in women with Addison's disease. *Clin Endocrinol (Oxf)* 52: 775–780.
32. Gurnell EM, Chatterjee VK (2001) Dehydroepiandrosterone replacement therapy. *Eur J Endocrinol* 145: 103–106.
33. Legrain S, Massien C, Lahlou N, Roger M, Debuire B, Diquet B, Chatellier G, Azizi M, Faucounau V, Porchet H, Forette F, Baulieu EE (2000) Dehydroepiandrosterone replacement administration: pharmacokinetic and pharmacodynamic studies in healthy elderly subjects. *J Clin Endocrinol Metab* 85: 3208–3217.
34. Lovas K, Gebre-Medhin G, Trovik TS, Fougner KJ, Uhlving S, Nedrebo BG, Myking OL, Kampe O, Husebye ES (2003) Replacement of dehydroepiandrosterone in adrenal failure: no benefit for subjective health status and sexuality in a 9-month, randomized, parallel group clinical trial. *J Clin Endocrinol Metab* 88: 1112–1118.
35. Munarriz R, Talakoub L, Flaherty E, Gioia M, Hoag L, Kim NN, Traish A, Goldstein I, Guay A, Spark R (2002) Androgen replacement therapy with dehydroepiandrosterone for androgen insufficiency and female sexual dysfunction: androgen and questionnaire results. *J Sex Marital Ther* 28: 165–173.
36. Villareal DT, Holloszy JO, Kohrt WM (2000) Effects of DHEA replacement on bone mineral density and body composition in elderly women and men. *Clin Endocrinol (Oxf)* 53: 561–568.
37. Leblanc M, Labrie C, Belanger A, Candas B, Labrie F (2003) Bioavailability and pharmacokinetics of dehydroepiandrosterone in the cynomolgus monkey. *J Clin Endocrinol Metab* 88: 4293–4302.
38. Davidson M, Marwah A, Sawchuk RJ, Maki K, Marwah P, Weeks C, Lardy H (2000) Safety and pharmacokinetic study with escalating doses of 3-acetyl-7-oxo-dehydroepiandrosterone in healthy male volunteers. *Clin Invest Med* 23: 300–310.
39. Villareal DT, Holloszy JO (2004) Effect of DHEA on abdominal fat and insulin action in elderly women and men: a randomized controlled trial. *JAMA* 292:2243–2248.
40. Segal KR, Landt M, Klein S (1996) Relationship between insulin sensitivity and plasma leptin concentration in lean and obese men. *Diabetes* 45: 988–991.
41. Slowinska-Srzednicka J, Zgliczynski S, Ciswicka-Sznajderman M, Srzednicki M, Soszynski P, Biernacka M, Woroszylska M, Ruzyllo W, Sadowski Z (1989) Decreased plasma dehydroepiandrosterone sulfate and dihydrotestosterone concentrations in young men after myocardial infarction. *Atherosclerosis* 79: 197–203.
42. Leal AM, Magalhaes PK, Souza CS, Foss NT (2003) Adrenocortical hormones and interleukin patterns in leprosy. *Parasite Immunol* 25: 457–461.
43. Villareal DT, Holloszy JO (2004) Effect of DHEA on abdominal fat and insulin action in elderly women and men: a randomized controlled trial. *JAMA* 292: 2243–2248.

DEVELOPMENTAL DYNAMICS 236:2865–2874, 2007

Genetic Interactions Between Activin Type IIB Receptor and Smad2 Genes in Asymmetrical Patterning of the Thoracic Organs and the Development of Pancreas Islets

Yutaka Goto,[1†] Masatoshi Nomura,[1*†] Kimitaka Tanaka,[1] Akiyo Kondo,[1] Hidetaka Morinaga,[1] Taijirou Okabe,[1] Toshihiko Yanase,[1] Hajime Nawata,[1] Ryoichi Takayanagi,[1] and En Li[2‡]

Signaling through activin type IIB receptor (ActRIIB) has been shown to regulate the axial formation and the development of foregut-derived organs such as the pancreas in mice. Here, we provide genetic evidence that ActRIIB and Smad2 genes cooperatively regulated asymmetrical patterning of the thoracic organs and pancreas development in mice. The loss of one allele of Smad2 on ActRIIB$^{-/-}$ background resulted in the increased severity of ActRIIB$^{-/-}$ phenotypes, including right pulmonary isomerism and complex cardiac malformations, and resulted in 100% frequency of death soon after birth. Of interest, 14% of compound heterozygous ActRIIB$^{+/-}$Smad2$^{+/-}$ mice exhibited the ActRIIB$^{-/-}$ phenotypes and died soon after birth. In the pancreas, hypoplastic islets were found not only in ActRIIB$^{-/-}$ but also in Smad2$^{+/-}$ mice. A more severe phenotype was also found in ActRIIB$^{+/-}$Smad2$^{+/-}$ mice. As well, these mutant mice exhibited impaired glucose tolerance in a gene dosage-sensitive manner. This genetic evidence strongly suggested that ActRIIB and Smad2 function in the same signaling pathway to regulate axial patterning and pancreas islet formation by means of a threshold mechanism. *Developmental Dynamics 236:2865–2874, 2007.*

Key words: activin receptor type IIB; Smad2; pancreas islet; left–right asymmetry; diabetes

Accepted 20 July 2007

INTRODUCTION

The transforming growth factor-β (TGF-β) family ligands exert a diverse range of biological effects on cell growth and differentiation (Mathews, 1994). TGF-β signals are mediated by binding to their cell surface serine/threonine kinase type II receptors. Activated type I receptors propagate the signal to specific intracellular Smad proteins, namely Smad2 and/or Smad3. Once phosphorylated, the receptor-regulated Smads (R-Smads) dissociate from the receptor complex, bind to a Co-Smad (Smad4), and enter the nucleus as a complex where they participate in the transcriptional regulation of the target genes (Derynck and Feng, 1997; Heldin et al., 1997; Massague and Chen, 2000). To date, more than 27 TGF-β family ligands have been identified in human (Venter et al., 2001), whereas only five type II receptors have been identified in mammals, suggesting overlapping receptor usage by TGF-β family ligands.

[1]Department of Medicine and Bioregulatory Science, Graduate School of Medical Sciences, Kyushu University, Higashi-ku, Fukuoka, Japan
[2]Cardiovascular Research Center, Massachusetts General Hospital East, Department of Medicine, Harvard Medical School, Charlestown, Massachusetts
Grant sponsor: the Japan Society for Promotion of Science Grant; Grant sponsor: Japan Science and Technology Corporation; Grant sponsor: Takeda Science Foundation.
†Drs. Goto and Nomura contributed equally to this work.
‡Dr. Li's present address is Novartis Institute for Biomedical Research, Cambridge, Massachusetts 02139.
***Correspondence to: Masatoshi Nomura, MD, PhD, Department of Medicine and Bioregulatory Science, Graduate School of Medical Sciences, Kyushu University, 3-1-1 Maidashi, Higashi-ku, Fukuoka 812-8582, Japan.**
E-mail: nomura@med.kyushu-u.ac.jp

DOI 10.1002/dvdy.21303
Published online 7 September 2007 in Wiley InterScience (www.interscience.wiley.com).

Two related type II receptors, ActRIIA and ActRIIB, have been initially identified as the type II receptors for activins (Attisano et al., 1992; Mathews, 1994). In addition to activins, ActRIIA and ActRIIB have subsequently been shown to bind to other TGF-β family proteins, including BMP7, Nodal, GDF8/Myostatin, and GDF11/BP11 (Yamashita et al., 1995; Lee and McPherron, 2001; Yeo and Whitman, 2001; Oh et al., 2002). The precise roles of the different activin receptors and Smads are still unclear, but they may be ligand and/or cell-type specific. The different usage of the type I and type II receptors and Smads may be one of the mechanisms for the different actions of TGF-β family on different tissues and target genes, explaining their functional diversity. Thus, the delineation of the cellular components of the system is necessary for understanding the regulation of numerous biological systems.

The type II activin receptors, ActRIIA and ActRIIB, have been shown to play important roles in axial patterning (Oh and Li, 1997; Song et al., 1999; Oh et al., 2002) and later in organ development (Oh and Li, 1997; Kim et al., 2000). The ActRIIA-deficient mice exhibit craniofacial defects including hypoplasia of mandibles, reduced fertility, and gastrulation defects (Matzuk et al., 1995; Song et al., 1999). On the other hand, the ActRIIB-deficient mice displayed multiple patterning defects, including complex cardiac defects, pulmonary isomerism (disturbance of left–right asymmetry), kidney agenesis, and axial patterning such as anterior transformation of the axial skeleton. Seventy percent of the ActRIIB$^{-/-}$ mice on hybrid background die after birth owing to right isomerism, which is characterized by mirror-image symmetrical right lungs, and complex cardiac malformations (Oh and Li, 1997). Although disruption of individual type II activin receptors results in nonoverlapping phenotypes, most of the phenotypes described for ActRIIA or ActRIIB mice exhibit incomplete penetrance and these two receptors show functional compensation during such patterning events. Type II activin receptors are broadly expressed in the mid-gestation mouse embryo, including in the pancreatic epithelium (Manova et al., 1995; Verschueren et al., 1995), and later are expressed in adult islets (Yamaoka et al., 1998). Pancreatic expression of a dominant-negative type II activin receptor in transgenic mice results in islet hypoplasia (Yamaoka et al., 1998; Shiozaki et al., 1999). The mice harboring null mutations in ActRIIA and ActRIIB such as ActRIIA$^{+/-}$ ActRIIB$^{+/-}$ and ActRIIB$^{-/-}$ exhibit hypoplastic pancreas islets and impaired glucose tolerance (Kim et al., 2000). These results suggest important roles of signaling through activin type II receptors in pancreas islet development and function.

Although type II activin receptors are shown to regulate the axial patterning and pancreas islet formation, an involvement of Smad proteins in the signaling pathway regulating these developmental processes remains elusive. Phenotypic comparison and genetic crosses of receptor-deficient mice and Smad-deficient mice should provide information to define in vivo interactions with these signaling partners. It has been shown that double heterozygous mice for nodal and Smad2 exhibit similar laterality defects seen in ActRIIB$^{-/-}$ mice, suggesting that nodal may signal through ActRIIB and Smad2 during thoracic organ patterning (Nomura and Li, 1998). With regard to pancreas islet development, GDF11-deficient mice have been shown to exhibit hypoplasia of the islet, due to the defect in β cell maturation, reminiscent of the phenotype found in Smad2$^{+/-}$ mice, suggesting that GDF11 uses Smad2 as a downstream signal transducer (Harmon et al., 2004). We thus speculated that Smad2 acts downstream to ActRIIB in these developmental processes, such as left–right patterning and pancreas development. As Smad2 functions in a dosage-sensitive manner (Nomura and Li, 1998), we predicted that a reduction of the gene dosage of Smad2 in ActRIIB mutant mice would result in an increased severity of the phenotypes in ActRIIB$^{-/-}$ mice. In this study, we generated mice carrying mutations of both ActRIIB and Smad2 genes. We found that the incidence of cardiac malformation and right pulmonary isomerism was significantly increased in ActRIIB$^{-/-}$Smad2$^{+/-}$ mice compared with ActRIIB$^{-/-}$ mice. In addition, we demonstrated that hypoplastic islets were found not in only ActRIIB$^{-/-}$ but also Smad2$^{+/-}$ mice, which was consistent with previous studies (Kim et al., 2000; Harmon et al., 2004). Interestingly, more severe phenotypes were found in the compound heterozygous ActRIIB$^{+/-}$ Smad2$^{+/-}$ mice. In addition, these mutant mice exhibited impaired glucose tolerance in a gene dosage manner. In conclusion, we provide compelling genetic evidence that Smad2 interacts with ActRIIB in axial development as well as pancreas islet development, suggesting that ActRIIB and Smad2 may function in the same signaling pathway in these developmental processes.

RESULTS

Genetic Interaction Between Type IIB Activin Receptor and Smad2 in Left–Right Patterning of Embryos

As previously described, Smad2 showed a haploinsufficiency in craniofacial development, suggesting that Smad2 functions in a dosage-sensitive manner (Nomura and Li, 1998). We therefore predicted that a reduced gene dosage of Smad2 in ActRIIB mutant mice would result in an increased penetrance or severity of the phenotypes in ActRIIB$^{-/-}$ mice. To elucidate the genetic interaction between ActRIIB and Smad2, we generated mice heterozygous for Smad2 and homozygous for ActRIIB (i.e., ActRIIB$^{-/-}$Smad2$^{+/-}$). To generate these mice, ActRIIB$^{+/-}$Smad2$^{+/-}$ mice were crossed with the ActRIIB$^{-/-}$ mice. The ActRIIB$^{+/-}$ mice were revealed to be normal and viable, whereas 20% of Smad2$^{+/-}$ mice and 70% of ActRIIB$^{-/-}$ mice on a hybrid genetic background die during gastrulation and perinatal stages, respectively. Therefore, according to the Mendelian ratio, we would expect four genotypes at an expected frequency shown in Table 1 in parentheses if there is no interaction between the two genes. However, as we expected, none of the ActRIIB$^{-/-}$ Smad2$^{+/-}$ mice were recovered at the weaning stage, as shown in Table 1. Because the lethality of the mice homozygous for ActRIIB was 74%, consistent with previous observation (Oh and

TABLE 1. Summary of the Genotypes of Offsprings from the Crosses between ActRIIB$^{+/-}$Smad2$^{+/-}$ and ActRIIB$^{-/-}$ at a Weaning Stage

ActRIIB$^{+/-}$Smad2$^{+/-}$ × ActRIIB$^{-/-}$			
Genotype		Weaning Stage	
ActRIIB	Smad2		
+/-	wt	53	(1.0)
+/-	+/-	35	(0.8)
-/-	wt	14	(0.3)
-/-	+/-	0	(0.24)
total		102	

Total litters, 22; average pups/litter, 4.6.

Li, 1997), the loss of one allele of Smad2 on ActRIIB homozygous background resulted in increased lethality, showing apparent genetic interactions of Smad2 and ActRIIB. It is noted that the ActRIIB$^{+/-}$Smad2$^{+/-}$ mice are less viable than expected, further suggesting genetic interaction between ActRIIB and Smad2. In ActRIIB homozygous mice, 70% of the mice die in the perinatal period due to laterality defects including abnormality in the cardiac outflow tracts. None of the ActRIIB$^{-/-}$ embryos showed gastrulation defects but died during gestation. Therefore, newborn mice from the crosses of ActRIIB$^{+/-}$Smad2$^{+/-}$ with ActRIIB$^{-/-}$ were dissected, and we analyzed the internal organs (Table 2). Of interest, all the mice with the ActRIIB$^{-/-}$Smad2$^{+/-}$ genotype, without exception, exhibited right pulmonary isomerism in addition to the cardiac outflow defects. In wild-type mice, the right lung has four lobes, including cranial (crl), medial (ml), caudal (cal), and accessory lobes (al), whereas the left lung has one lobe (LL; Fig. 1A). However, in the mice with the ActRIIB$^{-/-}$Smad2$^{+/-}$ genotype, the left lung also had four lobes, in mirror image to the right lung (Fig. 1B). This symmetrical lung lobation is known as right pulmonary isomerism (RPI). In addition, we often found the stomach in the thoracic cavity in the ActRIIB$^{-/-}$Smad2$^{+/-}$ embryos (Fig. 1C). In a wild-type heart, the pulmonary trunk (PT) is located anterior to and to the right of the aorta (Ao) and crosses over to the left of the Ao (Fig. 1D). In the mutant heart, the Ao arose from the anterior-most position of the heart, where the PT was located in the wild-type, whereas the PT was located posterior to, and on the right side of, the Ao (Fig. 1E) This abnormality of the outflow tract is similar to the human congenital heart defect known as transposition of the great artery (TGA) or double outlet right ventricle (DORV). Furthermore, the mutant mouse showed abnormal looping of the descending Ao as shown in Figure 1F. The descending Ao looped toward the right side, instead of looping to the left as in the wild-type mice (Fig. 1D). This opposite looping of the descending Ao was only found in ActRIIB$^{-/-}$ mice on 129/Sv background. These results clearly demonstrated that the loss of one Smad2 allele increases the penetrance and severity of the ActRIIB homozygous phenotype, because none of the Smad2 heterozygous mice show laterality defects. Moreover, of the 22 trans-heterozygous mice, 3 showed cardiac outflow defects, although none of the heterozygous mice showed any defects. Collectively, these results suggest that ActRIIB and Smad2 may function in the same signaling pathway to regulate such patterning events. The wild-type mice usually have seven ribs attached to the sternum, whereas ActRIIB$^{-/-}$ mice had nine ribs at 100% penetrance. We found that 3 of the 22 ActRIIB$^{+/-}$Smad2$^{+/-}$ mice had nine ribs, and characteristics similar to ActRIIB$^{-/-}$ mice (data not shown). None of the ActRIIB$^{+/-}$ nor Smad2$^{+/-}$ mice had nine ribs. Taken together, the increased penetrance and severity of the defects in addition to a new emergence of the phenotype characteristics of ActRIIB$^{-/-}$ in ActRIIB$^{+/-}$Smad2$^{+/-}$, suggesting that both ActRIIB and Smad2 reside in the same signaling pathway to regulate body pattern formation.

Hypoplasia of Pancreas in ActRIIB$^{-/-}$Smad2$^{+/-}$ Mice

Because ActRIIB$^{-/-}$Smad2$^{+/-}$ mice die after birth as described above, the embryos from the crosses between ActRIIB$^{+/-}$Smad2$^{+/-}$ and ActRIIB$^{+/-}$ mice were dissected and we analyzed the abdominal organs before birth at embryonic day (e) 18.5. ActRIIB$^{+/-}$, ActRIIB$^{-/-}$, Smad2$^{+/-}$ and ActRIIB$^{+/-}$ Smad2$^{+/-}$ embryos displayed no detectable malformations of the visceral organs, whereas some of the ActRIIB$^{-/-}$ Smad2$^{+/-}$ embryos displayed abdominal organ heterotaxy in addition to thoratic heterotaxy, as described above. The weights of the pancreas from the embryos with each genotype were measured as shown in Figure 2A. The weights of pancreas from the ActRIIB$^{-/-}$Smad2$^{+/-}$ mice were reduced by approximately half compared with those of mice with the other genotypes, although there was no difference in their body weights. Because the activin signaling is implicated in the endocrine cell specification, insulin contents of the whole pancreases were measured by the acid–ethanol method. As shown in Figure 2B, insulin content in the pancreata of ActRIIB−/− Smad2$^{+/-}$ mice was significantly reduced. Interestingly, the insulin content in the pancreata of ActRIIB+/− Smad2$^{+/-}$ mice was dramatically reduced by half compared with that of wild-type mice. These results suggest that the signaling by ActRIIB-Smad2 plays an important role not only in pancreas development but also islet development. However, islet β-cell formation may be more sensitive to the signal through ActRIIB-Smad2 than exocrine pancreas development. Furthermore, there might be a threshold mechanism in the signaling that is required for specific organ development.

Defective Islet Formation in ActRIIB$^{-/-}$Smad2$^{+/-}$ Mice

Reduced insulin content and hypoplasia of the pancreata in the ActRIIB$^{-/-}$ Smad2$^{+/-}$ mice prompted us to analyze the histology of the pancreas. Sagittal sections of wild-type and ActRIIB$^{-/-}$ Smad2$^{+/-}$ embryos at e18.5 are shown in Figure 3, upper and lower panels, respectively. The embryo with the ActRIIB$^{-/-}$Smad2$^{+/-}$ genotype displayed